ResearchGate

See discussions, stats, and author profiles for this publication at: https://www.researchgate.net/publication/7021612

SRY-directed DNA Bending and Human Sex Reversal: Reassessment of a Clinical Mutation Uncovers a Global Coupling between the HMG Box and its Tail

ARTICLE *in* JOURNAL OF MOLECULAR BIOLOGY · AUGUST 2006

Impact Factor: 4.33 · DOI: 10.1016/j.jmb.2006.04.048 · Source: PubMed

CITATIONS
15

READS
27

8 AUTHORS, INCLUDING:

Biaoru Li

39 PUBLICATIONS **476** CITATIONS

SEE PROFILE

Elisha Haas

Bar Ilan University

100 PUBLICATIONS **2,901** CITATIONS

SEE PROFILE

Available from: Biaoru Li
Retrieved on: 28 January 2016

doi:10.1016/j.jmb.2006.04.048 J. Mol. Biol. (2006) 360, 310–328

JMB

Available online at www.sciencedirect.com

SCIENCE DIRECT®

ELSEVIER

SRY-directed DNA Bending and Human Sex Reversal: Reassessment of a Clinical Mutation Uncovers a Global Coupling between the HMG Box and its Tail

Biaoru Li[1]†, Nelson B. Phillips[1]†, Agnes Jancso-Radek[1] Varda Ittah[2], Rupinder Singh[1], David N. Jones[1] Elisha Haas[2] and Michael A. Weiss[1]*

[1]*Department of Biochemistry Case School of Medicine, Case Western Reserve University Cleveland, OH 44106-4935 USA*

[2]*Faculty of Life Sciences, Bar Ilan University, Ramat Gan Israel 52900*

**Corresponding author*

Sex-reversal mutations in human SRY cluster within its high-mobility group box, a conserved motif of DNA bending. A classical substitution at the crux of this angular domain (M64I) has been reported to impair DNA bending but not DNA binding, implying that sharp bending is required for transcriptional activation and testis determination. Surprisingly, we report that this defect was an inadvertent consequence of protein truncation: in the intact protein, sharp DNA bending is restored by the basic tail of the high-mobility group box. Structural coupling between box and tail is tuned to the native DNA bend angle, damping conformational fluctuations and enabling bidirectional induced fit within the bent complex. M64I-associated sex reversal is instead caused by the impaired function of a flanking non-classical nuclear localization signal (NLS). Similar impairment is caused by M64A, suggesting that mislocalization is due to loss of an M64-specific function and not gain of a non-native I64-specific function. Transcriptional activity, attenuated by mislocalization, is rescued by fusion of a heterologous NLS. In a male embryonic gonadal cell line, M64I and M64A SRY-NLS fusion proteins exhibit native transcriptional activation of *Sox9*, a key step in testicular differentiation. Our results suggest that male development is robust to subtle alterations in SRY-DNA architecture but depends critically on nuclear localization. The previously unsuspected role of M64 within a non-classical NLS may contribute to its invariance among SOX-related and LEF-1-related transcription factors.

© 2006 Elsevier Ltd. All rights reserved.

Keywords: gene regulation; protein structure; intersex abnormalities; gonadal dysgenesis; human development

Introduction

The male phenotype in eutherian mammals is determined by *Sry*, a gene on the Y chromosome.[1] SRY contains a high-mobility group (HMG) box (Figure 1(a)),[2] a conserved motif of DNA binding and DNA bending.[3] Its assignment as the testis-determining factor is supported by studies of

† B.L. and N.B.P. contributed equally to this work.

Present addresses: A. Jancso-Radek, Epicentre Technologies, Madison, WI 53713, USA; D.N. Jones, University of Colorado Health Sciences Center, Denver, CO, USA.

Abbreviations used: 6-FAM, 6-isomer of acetamido-fluorescein; CaM, calmodulin; FRET, fluorescence resonance energy transfer; HMG, high mobility group; GMSA, gel mobility-shift assay; LEF-1, lymphoid enhancer factor 1; MIS, Mullerian inhibiting substance (also called anti-Mullerian hormone); NLS, nuclear localization signal; PGE, permutation gel electrophoresis; rp-HPLC, reverse-phase HPLC; HSQC, heteronuclear single quantum coherence; RT-Q-rtPCR, real-time PCR assay; SOX, SRY-related HMG box; SRY, protein encoded by sex-determining region of Y chromosome; SRY-p and SRY-p_{Δ}, domains containing residues 2–86 and 2–78, respectively; TAMRA, tetramethylrhodamine; TBP, TATA-binding protein; TCF-1α, T-cell factor 1α and homologue of LEF-1; X-gal, 5-bromo-4-chloro-3-indolyl-β-D-galactosidase.

E-mail address of the corresponding author: michael.weiss@case.edu

0022-2836/$ - see front matter © 2006 Elsevier Ltd. All rights reserved.

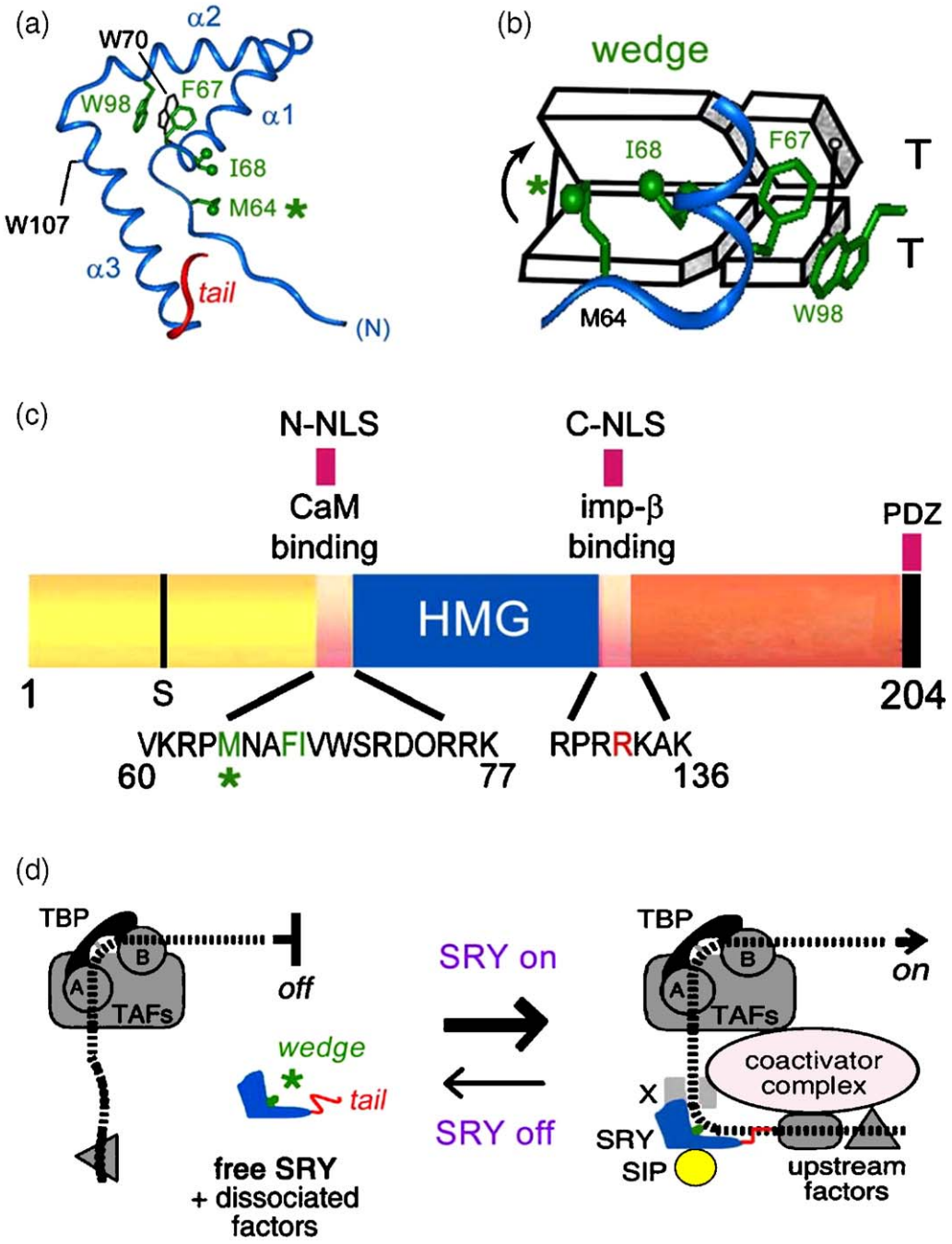

Figure 1. SRY and the enhanceosome model of gene regulation. (a) Ribbon model of SRY HMG box. The L-shaped structure contains the major wing (consisting of α-helix 1, α-helix 2, the first turn of α-helix 3, and connecting loops) and the minor wing (the N-terminal β-strand, the remainder of α-helix 3, and C-terminal tail). Selected side-chains are labeled; the asterisk (*) indicates M64. The hydrophobic wedge (M64, F67, I68, and W98) is shown in green, and the proximal portion of the tail is shown in red. (b) Wedge interactions with AT base-pairs disrupt base-stacking but not base-pairing; I68 partially intercalates as a ''cantilever'' side-chain. (c) Domains of intact SRY: nuclear localization signals N-NLS and C-NLS, respectively proposed to interact with calmodulin[38,39] and importin-β respectively.[36] Wedge residues M64 (asterisk), F67 and I68 are shown in green; sex-reversal site R133 shown in in red. In the N-terminal non-box region, S indicates the potential phosphorylation site proposed to modulate DNA binding;[75] the extreme C terminus contains a PDZ-binding motif, which interacts with SIP-1.[76,77] (d) A model of SRY-directed assembly of a male-specific transcriptional preinitiation complex. The asterisk indicates the hydrophobic wedge. Right: activated transcription in the presence of the bent DNA–SRY complex (green).[78] Left: activated transcription is off in the absence of SRY due to disassembly of theh DNA–multiprotein complex. Putative factor X binds cooperatively with SRY to the adjoining DNA site.[63]

human intersex abnormalities (46, XY gonadal dysgenesis)[4–8] and transgenic murine models.[9] Selective conservation of the SRY HMG box as a sequence-specific DNA-bending motif[10] suggests that the protein functions as an architectural transcription factor.[2,11] This proposal is supported by clinical observations that almost all mutations causing sex reversal occur in the HMG box (Figure 1(c)) and impair specific DNA binding.[11,12] The central contribution of site-specific DNA bending to developmental gene regulation is further supported by studies of chimeric murine *Sry* (*mSry*) transgenes in XX mice.[13,14] Here, we investigate how a classical *de novo* sex-reversal mutation[4] affects the structure of human SRY and impairs SRY-directed transcriptional regulation. The mutation (M64I; position 9 in the HMG box) lies near the crux of the angular HMG box (Figure 1(a)) at one edge of a ''hydrophobic wedge'' of side-chains abutting the bent DNA site (Figure 1(b)).[15]

SRY belongs to the extensive SOX family of transcription factors, which play critical and diverse roles in vertebrate organogenesis.[16] Autosomal gene *Sox9*, for example, functions downstream of *Sry* in the testis-determining pathway.[17,18] Although direct targets of SRY-mediated regulation have not been characterized, expression profiling of murine pre-Sertoli gonadal cells has defined an extensive network of candidate downstream genes, including *Sox9*, *Desert hedgehog* (*Dhh*), *Fibroblast growth factor 9* (*Fgf9*), and *Prostaglandin D synthase* (*Ptgds*).[19] The developmental importance of this network is demonstrated by human genetics[20–23] and knock-out mice.[24–26] The marked effects of SRY on DNA structure[15] are proposed to contribute to the assembly of sex-specific transcriptional pre-initiation complexes (Figure 1(d)).[27–30] Studies of Sox9 further suggest that such factors can interact with a chromatin template to recruit coactivators associated with nucleosome modification.[31]

SRY is a nuclear protein.[32,33] Two nuclear localization signals (NLS) have been defined in cell culture and are jointly required (Figure 1(c)): a bipartite basic motif near the N terminus of the HMG box (N-NLS; residues ^{61}KRxxxxxxxxxRxxRR^{76}K in human SRY; consensus positions 6–21‡)[32] and a basic cluster in the C-terminal tail of the HMG box (C-NLS; residues ^{130}RPRRKA^{136}K in human SRY, consensus positions 75–81)[34,35] The C-NLS binds to importin β.[36] The physiological relevance of this interaction (and, more broadly, of nuclear localization itself) is demonstrated by sex-reversal mutation R133W: although compatible with native DNA binding and bending, the mutation impairs nuclear import[35] and blocks binding to importin β.[37] How N-NLS functions is not well understood. Despite its resemblance to a classical bipartite motif and the functional importance of basic residues,[32,38] N-NLS does not bind to importin α or β.[36] Although binding of N-NLS to calmodulin (CaM) has been described,[39] evidence for the role of CaM in the nuclear trafficking of SRY is indirect.[40] Corresponding N-NLS and C-NLS elements are conserved within the HMG boxes of SOX proteins[34]; analogous elements have been defined in LEF-1/TCF.[41]

In this study, we reinvestigate a classical mutation in SRY (M64I) originally reported to impair specific DNA bending without significant effects on DNA binding.[42] Such discordance between bending and binding, unique among sex-reversal mutations to our knowledge, has been cited widely as evidence for a strict relationship between DNA bend angle and SRY activity.[40] The structural basis of impaired DNA bending has itself attracted considerable interest.[43] NMR studies have revealed a key perturbation in DNA bending due to the absence of the M64 sulfur atom and associated M64-R72 hydrogen bond, part of a brace abutting splayed AT base-pairs at the site of I68 cantilever insertion (Figure 2).[43] Surprisingly, we demonstrate that the original DNA-bending defect[42] was a consequence of truncation of the HMG box and is not a property of the intact protein. Further, the decrement in DNA bending observed in the structural studies[43] was exaggerated by use of a non-consensus DNA sequence. Essentially native DNA bending is restored by inclusion of the C-terminal basic tail of the HMG box (red segments in Figure 2(a) and (b)) and use of a consensus DNA target site. Tail-dependent restoration of DNA bending is associated with damping of conformational fluctuations, revealing a non-local structural coupling within the bent SRY–DNA complex. As a further surprise, our results suggest that M64I-associated sex reversal is caused by a cryptic defect in nuclear import. Rescue of nuclear localization by a heterologous NLS[44] restores native gene-regulatory properties in a cell-culture model of testis-specific Sertoli cell differentiation. We propose that the broad conservation of M64 among SRY, SOX, and LEF-1 factors is enjoined by its previously unsuspected role in a non-classical NLS.

Results

This study employs intact human SRY (204 amino acid residues) and two DNA-binding domains (residues 57–141 and 57–133). The domains (designated SRY-p and SRY-p_Δ), corresponding to residues 2–86 and 2–78 in a consensus HMG box, differ in the length of the C-terminal tail.[15,43] The DNA-bending properties of SRY-p are similar to those of full-length SRY,[11,45] whereas SRY-p_Δ exhibits twofold lower specific DNA affinity and somewhat attenuated DNA bending.[46] The defective DNA-bending properties of M64I SRY were originally described in the context of SRY-p_Δ.[42] Wild-type (wt) and M64I domains of either length exhibit similar CD,

‡ Amino acids are designated by standard codes. Residue numbers in SRY refer to intact human SRY unless otherwise indicated. Consensus position 1 in the HMG box corresponds to residue 57 of the intact human SRY.

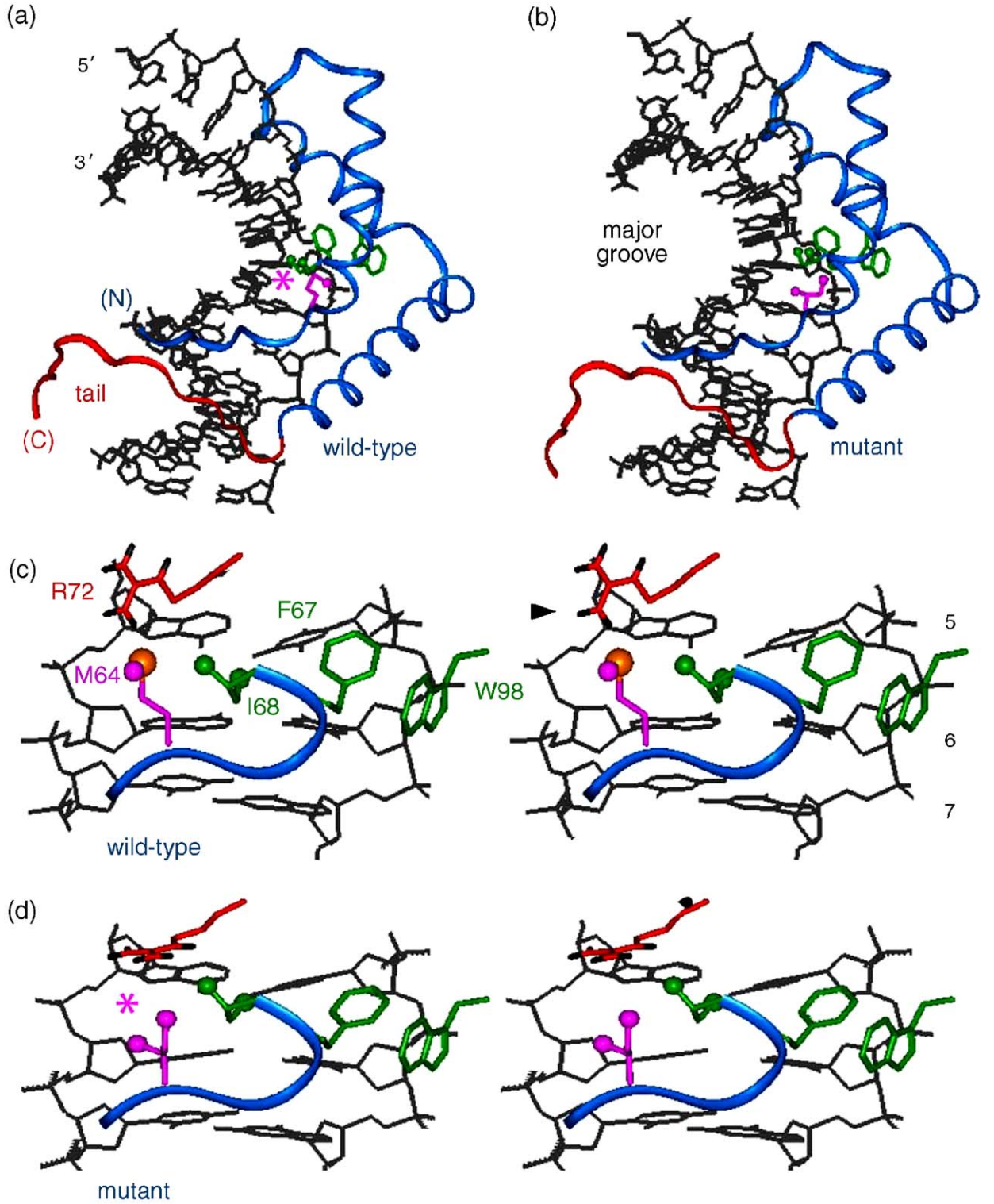

Figure 2. Structures of SRY–DNA complexes. (a) and (b) Wild-type and M64I SRY–DNA complexes bound to the variant DNA site (core sequence 5′-TTTGTG-3′ and complement).[43] In each case, the protein ribbon is in blue (HMG box) and red (tail; residues 125–140 in human SRY and HMG positions 70–85); hydrophobic wedge side-chains (M64, F67, I68, and W98; positions 9, 12, 13, and 43 in HMG box) are shown in green; and DNA is shown as gray sticks. (c) and (d) Stereo pairs showing wedge–DNA interactions surrounding M64 ((c) wild-type) and I64 ((d) mutant) in respective protein–DNA structures. The arrowhead indicates R72 (position 17 in HMG box), whose guanidium group hydrogen bonds to the sulfur atom (gold) of M64 ((c)); (d) this interaction is absent and R72 displaced in variant structure. The coordinates were obtained from the Protein Databank (accession codes **1J46** and **IJ47**, respectively).

tryptophan fluorescence, and ^{1}H-NMR spectra, indicating that the mutation does not perturb the structure of the free domain. Thermal and denaturant-induced unfolding transitions likewise yield similar estimates of stability; the thermal stability of M64I SRY-p is 3 deg. C greater than that of wt SRY-p (Supplementary Data). Analysis of specific DNA binding by the gel mobility-shift assay (GMSA) and a fluorescence resonance energy transfer (FRET)-based equilibrium binding assay[46] demonstrate that the binding of the mutant protein is 2.5-fold weaker than that of the wild-type in accord with the results of previous studies.[42] This fold-decrement in not affected by truncation of the tail of the HMG box. Specific binding of a control M64A analog is similar to that of M64I, whereas its thermal stability is 2 deg. C lower than that of the wt domain.

Mutation does not perturb DNA bending in the presence of the basic tail

Analysis of DNA bending by permutation gel electrophoresis (PGE) demonstrates that the marked DNA-bending defect originally ascribed to M64I in SRY-p$_{\Delta}$ ($\Delta\theta$ 18°)[42] is reproducible (Figure 3(a) and line 3 in Table 1, bold). By contrast, the effect of the mutation is very small in the context of the intact protein or SRY-p ($\Delta\theta$ 2–3°; Figure 3(b) and Table 1). Consensus DNA sites (5′-ATTGTT-3′ and complement) were characterized in three sequence contexts (sites 1–3 in Table 1); these sites correspond to probes previously employed by others.[42,47,48] Binding of an intact tail thus restores near-native DNA bending to the mutant HMG box. Conversely, whereas the bend angle of the wt SRY-p complex is only modestly perturbed by truncation of the tail ($\Delta\theta$ 7–10°),[46] truncation of the M64I complex causes a 25° decrement in DNA bending (76° *versus* 51°, Table 1, rows 2 and 3 in column 5).

PGE analysis of non-consensus DNA sites 4 and 5 unmasks an M64I-associated bending defect in the presence of the tail (Table 1, rows 6–8). The variant sites each contain transversions within the core target site that impair DNA bending and binding.[49] Site 4 (5′-GTG**T**TTGT**G**CAG-3′; non-consensus bases in bold) was has been used in structural studies (Figure 2).[43] Comparison with parent site 1 (5′-GTGATTGTTCAG-3′) yields wt SRY-p/DNA bend angles of 79° (site 1) and 68° (site 4); the corresponding values in M64I-SRY-p complexes are 76° (site 1) and 62° (site 4). The M64I-associated decrement in a tailed site 4 complex ($\Delta\theta$ 6°) is thus twice as large as that observed with the consensus DNA site ($\Delta\theta$ 3°). A more extreme DNA dependence is observed on binding of the proteins to site 5 (5′-CCCATTG**A**TCTC-3′; transversion in bold) relative to parent site 2 (5′-CCCATTGTTCTC-3′). Binding of wt SRY-p to site 5 induces a bend angle of 68°, a decrement ($\Delta\theta$) of 19° relative to the consensus complex (site 2; Figure 3(c)). By contrast, binding of M64I SRY-p leads to a bend angle of only 42°, a decrement of 26° relative to wt SRY (Figure 3(d) and Table 1, row 8) and an extraordinary decrement of 37° relative to the consensus wt complex (Table 1, row 2). These observations suggest that the transversion in site 5 impairs binding of the tail, hence unmasking and accentuating the bending defect of the M64I HMG box. The structure of the wt SRY-site 4 complex[43] suggests that this transversion would perturb tail–DNA contacts.

Specific DNA bending was further characterized by fluorescence resonance energy transfer (FRET).[50,51] FRET provides a sensitive probe of bending, as end-to-end DNA distances are sensitive to mean bending (Figure 4(a))[45,51] and fluctuations in DNA bend angle (Figure 4(b)).[46] The DNA target site (site 1) was labeled with a donor (fluorescein; 6-FAM) at one 5′ end and/or an acceptor (tetramethylrhodamine; TAMRA) at the other 5′ end (Figure 4(a)).[45,48] Labeled DNA sites contain 15 bp and so span about 1.5 turns of the double helix; this geometry positions the donor and acceptor on the same side of the double helix (green and red balls in Figure 4(a)). Despite the marked changes in the DNA conformation upon binding by SRY, the structure of the SRY DNA complex as determined by NMR indicates that the two 5′-linked fluorophores would remain on one side of the bent complex.[52] Time-resolved fluorescence anisotropy measurements demonstrate that the shortest correlation-time components and its

Figure 3. PGE DNA-bending assays. M64I causes (a) a marked DNA- bending defect in the truncated fragment SRY-p$_{\Delta}$ but (b) negligible DNA-bending defect in the presence of the basic tail. In (a) and (b), the gel is shown at the left and analyses of mobilities at the right. Permutation probes contain consensus site 5′-GTG**ATTGTT**CAG-3′ (and complement; core target site in bold) in 146 bp probes. A plot is shown of relative mobility as a function of flexure displacement: wild-type (filled triangles) and mutant (filled squares). (a) PGE analysis of wt SRY-p$_{\Delta}$ (left-hand set) and M64I SRY-p$_{\Delta}$ (right-hand set). Inferred DNA bend angles are 71(±1)° (wild-type; filled triangles at the right) and 56(±1)° (mutant; filled squares). (b) PGE analysis of wt SRY-p (left-hand set) and M64I SRY-p (right-hand set); inferred DNA bend angles are 79(±1)° and 76(±1)°. (c) and (d) Non-consensus DNA-bending assays. (c) DNA bending by wt SRY is reduced by A→T transversion in the DNA site (5-ATTG**A**T-3′; asterisk in (c)). Left: PGE analysis of wt SRY-p bound to the consensus DNA site (left-hand set) and wt SRY bound to the non-consensus DNA site (right-hand set). Right: plot of electrophoretic mobility as a function of flexure displacement: consensus complex (filled triangles; 5′-CC**ATTGTT**CT-3′ and complement); and non-consensus complex (open circles; CC**ATTGAT**CT-3′ and complement). Inferred DNA bend angles are 83(±1)° and 66(±1)°, respectively. (d) Bending of non-consensus DNA site is impaired by M64I mutation. Left, PGE analysis of M64I SRY (left-hand set) and wt SRY (right-hand set) bound to 5′-CC**ATTGAT**CT-3′ (and complement). Right: inferred DNA bend angles are 66(±1)° (consensus; filled triangles) and 42(±1)° (non-consensus; filled squares). (a) and (b) Gels contain 10% polyacrylamide (29:1 (w/w) acrylamide:bis-acrylamide); (c) and (d) gels contain 10% polyacrylamide (58:1 (w/w) acrylamide:bis-acrylamide).

pre-exponents are similar among the samples (Supplementary Data). Steady-state FRET measurement is shown in Figure 4(c); control spectra of sites containing only the donor (spectra Dn in Figure 4(c)) or only the acceptor (spectra Ac) demonstrate that binding of the SRY domains does not result in quenching of either fluorophore. The predominance of an intramolecular FRET mechanism in the double-labeled samples was verified by analysis of solutions containing an equimolar mixture of DNA sites labeled with only 6-FAM or TAMRA.[45]

In accord with the results of previous studies,[45,48] FRET efficiency is enhanced on protein binding (relative to a baseline FRET efficiency of 51.2 (±1) % in the free 15 bp DNA; blue spectrum in Figure 4(c)). In the presence of the tail, FRET efficiencies of wild-type and variant DNA complexes are indisti-

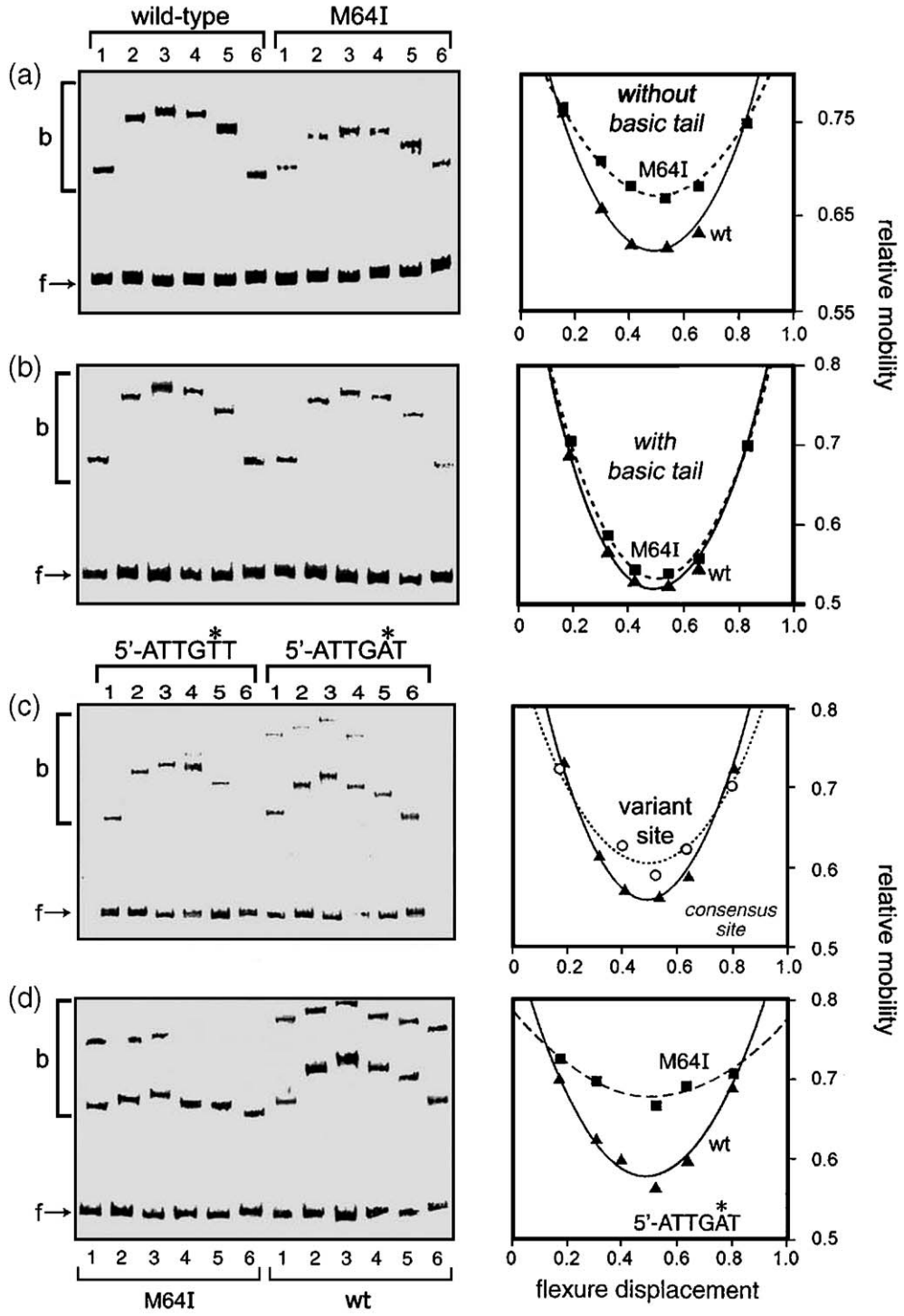

Figure 3 (*legend on previous page*)

Table 1. Electrophoretic DNA bend angles

Site [a]	Protein [b]	θ (°)	Protein	θ (°)	Δθ (°) [c]
1 (5′-gtgATTGTTcag)	wt SRY	80	M64I SRY	77	3
1	SRY-p	79	M64I SRY-p	76	3
1	SRY-p_Δ	69	M64I SRY-p_Δ	51	**18**
2 (5′-cccATTGTTctc)	SRY-p	87	M64I SRY-p	85	2
3 (5′-cgcATTGTTatc)	SRY-p	84	M64I SRY-p	82	2
4 (5′-gtgTTTGTGcag)	SRY-p	68	M64I SRY-p	62	6
4	wt SRY-p_Δ	49	M64I SRY-p_Δ	ND	ND
5 (5′-cccATTGATctc)	SRY-p	68	M64I SRY-p	42	26
1 (5′-gtgATTGTTcag)	SRY-p	79	M64A SRY-p	77	2
2 (5′-cccATTGTTctc)	SRY-p	87	M64A SRY-p	86	1
3 (5′-cgcATTGTTatc)	SRY-p	84	M64A SRY-p	83	1

Values shown (±1°) are referenced to the inferred DNA bend angle of SRY-p complexes as run at 4 °C in 10% polyacrylamide gel (28:1 (w/w) acrylamide:bis-acrylamide). ND, not determined. For samples run in gels of different composition (in which estimates of absolute bend angles may vary), Δθ values were determined on the basis of wild-type and variant complexes run side-by-side in the same gel.

[a] Sites 1, 2 and 3[42,47,48] contain the canonical high-affinity target sequence 5′-ATTGTT-3′ and complement. Site 4 is the MIS site employed in structural studies (Figure 2),[43] whereas site 5 is a variant of site 2.

[b] wt and M64I SRY designate full-length wild-type and variant proteins, respectively; SRY-p, residues 56–140; and SRY-p_Δ, residues 56–133.

[c] Δθ is defined as the difference in bend angle between the wt complex (column 3) and the mutant complex (column 5).

nguishable: 68.3(±1) % (wt SRY-p complex; yellow spectrum in Figure 4(c)) and 68.0(±1) % (M64I SRY-p complex; superimposed red dots in Figure 4(c)). On truncation of the tail, efficiencies are reduced: 66.4(±1) % (wt SRY-p_Δ complex; spectrum not shown), and 63.8(±1) % (M64I SRY-p_Δ complex; olive green spectrum in Figure 4(c)). FRET efficiencies thus correlate with respective DNA bend angles. In further accord with PGE results are the reduced FRET efficiencies in complexes containing site 4: 66.2(±1) % (wt SRY-p), 64.4(±1) % (M64I SRY-p), and 62.2(±1) % (M64I SRY-p_Δ complex). Thus, whereas M64I SRY-p exhibits native FRET efficiency when bound to a consensus DNA site in the presence of the tail, use of a non-consensus DNA site unmasks a FRET perturbation, which is accentuated on truncation of the tail.

Changes in mean DNA bend angle may, in principle, reflect static structural changes (model I in Figure 4(b)) or dynamic perturbations leading to conformational excursions (model II). These mechanisms can be distinguished by time-resolved measurements of the decay of donor fluorescence, which makes distance distribution analysis possible (Figure 4(d)).[53,54] Time-resolved FRET measurements demonstrate a significant change in donor lifetime in the double-labeled DNA site on binding of site 1 to SRY domains. Global analyses yield estimates of end-to-end distance distributions in the free and bound states (Figure 4(d) and Supplementary Data). On binding of wt SRY-p, the mean end-to-end distance of the DNA at 15 °C was reduced from 61.6 Å (61.5–61.7) (black gaussian distribution in Figure 4(d)) to 50.8 Å (50.3–51.2) (red distribution). Similarly, on binding of the M64I SRY-p, the mean distance was reduced to 50.9 Å (50.4–51.3) (green distribution), which is equivalent (within error) to the mean distance in the wt complex. By contrast, the mean distance in M64I SRY-p_Δ complex is 53.3 Å (52.7–53.5) (blue distribution). Although reductions of end-to-end distance can reflect both DNA bending and correlated changes in DNA unwinding, the predominant contribution is due to DNA bending.[45,51,55]

Skewed gaussian modeling of each protein–DNA complex indicates a significant broadening of end-to-end distributions relative to free DNA (the fitting and statistical parameters are provided in the Supplementary Data). Whereas the breadth of the distribution in the free DNA (~12.8 Å) is consistent with the allowed range of flexible linker configurations, the widths increase to 20.5 Å in the wt SRY-p complex and 22.4 Å in the corresponding M64I complex (Supplementary Data). Such broadening suggests that bound DNA structures exhibit a distribution of conformational substates and, in turn, a range of populated DNA bend angles. The truncated M64I complex exhibits a further increase in distribution width to 23.5 Å (Supplementary Data). Thus, on truncation of the tail, the M64I SRY-p_Δ complex exhibits perturbations in both mean DNA bending and dynamic stability, whereas in the M64I SRY-p complex the tail damps such aberrant conformational excursions. Such tail-specific damping was not observed in wt SRY–DNA complexes.[46]

The M64I SRY–DNA complex exhibits native tail-dependent NMR features

The SRY HMG box is flexible in the absence of DNA[56] and adopts a well-defined structure on specific DNA binding.[43,45,46] A signature of DNA-dependent stabilization is provided by 2D ^{1}H-^{15}N heteronuclear single quantum coherence (HSQC) spectra: the free domain exhibits limited chemical-shift dispersion and a mixture of major and minor cross-peaks (Supplementary Data), suggesting the presence of multiple conformations, whereas the DNA-bound domain exhibits a single predominant and well-resolved spectrum (Figure 5(a)). The tailed M64I SRY-p/site 1 complex exhibits a native-like

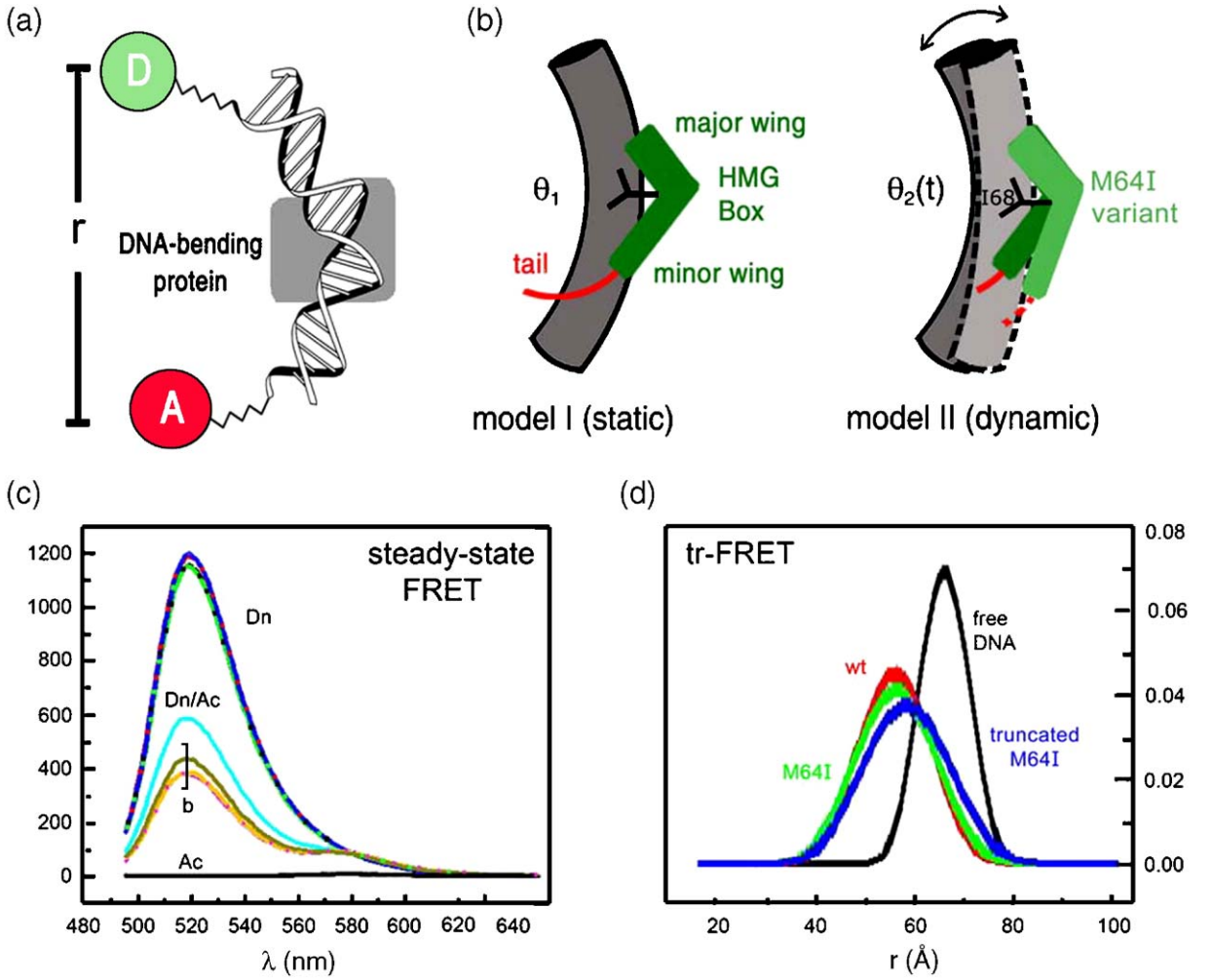

Figure 4. FRET studies of DNA bending. (a) Design of 15 bp DNA probe containing 5′-donor (6- FAM; green circle) on one strand and 5′-acceptor (TAMRA; red circle) on the other. A central bend would reduce the distance between the ends. (b) Static and dynamic models of impaired DNA bending: decreased mean bend angle in truncated M64I complex relative to tailed complexes may be due to a shift in set point (model I; middle panel) or conformational fluctuations (model II; right-hand panel). Bent DNA sites are shown in gray (cylinders), HMG boxes are shown in green, and tails are shown in red. The I68 cantilever is shown. The arrow in model II represents fluctuations in bend angle θ (*t*). (c) Emission spectra of free and bound DNA. (Dn) DNA singly labeled with fluorescein: black, free DNA; purple, wt SRY-p complex; powder blue, M64I SRY-p; green, M64I SRY-p$_\Delta$ complex (overlapping spectra). (Dn/Ac) Doubly labeled DNA: powder blue, free DNA; olive green, M64I truncated complex; yellow, wt SRY-p complex and magenta (circles), M64I SRY-p complex. (Ac) Emission spectra of DNA singly labeled with rhodamine (free DNA, complexes with wt SRY-p, M64I- and truncated M64I domains) overlap. (d) Gaussian models of end-to-end distances in free and bound DNA sites. End-to-end distance distributions of doubly labeled DNA in the free state (black) and as complexed; wt domain (red), M64I tailed domain (green) and M64I truncated domain (blue). Increased widths of the bound-state distributions, especially prominent in truncated M64I complex, reflect long-range conformational fluctuations.

HSQC spectrum (Figure 5(b) and Supplementary Data). This NMR ''fingerprint'' is not significantly perturbed on truncation of the wt tail (Figure 5(c)), whereas the truncated M64I complex exhibits a paucity of main-chain cross-peaks and large variation in line-widths (Figure 5(d)). Resonance assignment[43] indicates that residues at or near the DNA interface are preferentially broadened or absent as exemplified by Trp indole resonances (box in Figure 5(a)) and the side-chain carboxamide resonances of N65 (asterisk (*) in Figure 5(d)).

Probes of the bent DNA structure are provided by DNA ^{1}H-NMR imino resonances (Figure 6(a)). In the free DNA guanine imino resonances (base-pairs 2–4, 6, 10, and 13; numbering scheme inset in Figure 6(a)) are clustered between 12 ppm and 13 ppm, whereas thymidine resonances (base-pairs 5, 7–9, 11 and 12) are clustered between 13.4 ppm and 14.0 ppm (spectrum i). Addition of either wt or M64I SRY-p to form a specific 1:1 complex results in marked changes in chemical shifts (spectra ii and iii in Figure 6(a)). These complexes exhibit similar patterns of changes in chemical shift (''complexation shifts''; $\Delta\delta$). In each case, G10 is shifted upfield, for example, and T11 downfield. Further, insertion of cantilever side-chain I68 between T8

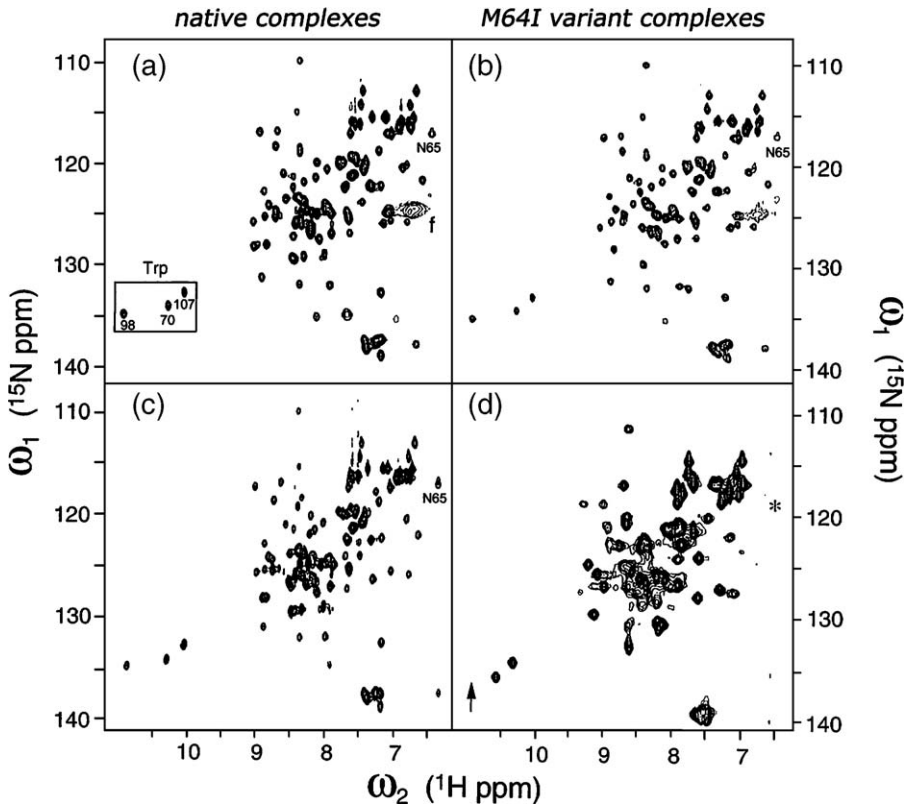

Figure 5. ^{1}H-^{15}N NMR HSQC footprints of protein–DNA complexes. (a) wt SRY-p tailed complex; (b) M64I SRY-p complex; (c) wt SRY-p_{Δ} complex; and (d) M64I SRY-p_{Δ} complex. These studies employed consensus DNA site 1. Spectra (a), (b) and (d) were acquired at 25 °C at 600 MHz; spectrum (c) was acquired at 400 MHz.

and T9 (boxed in the inset sequence in Figure 6(a)) is associated with an anomalous upfield shift of T8 into the guanine region (bracket above spectrum iii in Figure 6(a)).[57] Subtle differences in complexation shifts are nonetheless observed between the two complexes. In general, complexation shifts are slightly larger in the wt SRY-p complex than in the corresponding M64I complex (vertical continuous lines between spectra ii and iii in Figure 6(a)). By contrast, the chemical shifts of the Trp indole NH resonances are identical (vertical broken lines in Figure 6(a)). The upfield δ-CH_3 resonance of I68 (which inserts most deeply in the double helix)[43] is near –1.2 ppm in both complexes; this shift is slightly more upfield in the tailed wild-type complex (Δδ 0.04 ppm; Supplementary Data). The slight attenuation of the I68 complexation shift is similar in magnitude to that observed among imino DNA resonances.

Tail truncation causes only subtle changes in the ^{1}H-NMR spectrum of the wt complex: (spectra v and vi in Figure 6(b)).[46] These studies employed a 12 bp DNA site corresponding to positions 4–15 of the above 15mer (for convenience, the original numbering scheme is retained in spectra iv and v). Imino chemical shifts in the wt complex (spectrum v; 400 MHz) are similar to those in the 15 bp complex (spectrum ii; 600 MHz). By contrast, in the context of SRY-p_{Δ}, M64I causes a marked perturbation in ^{1}H-NMR features (spectrum vii in Figure 6(b)). Imino DNA resonances are broad and less shifted. The reduced DNA bend angle and aberrant breadth of the FRET-derived end-to-end distance distribution characteristic of the truncated M64I complex (Table 1 and Supplementary Data) suggest that these anomalous ^{1}H-NMR features reflect millisecond motions leading to enhanced fluctuations in DNA bend angle and ^{1}H-NMR conformational broadening. The indole resonances of W70 and W98 are likewise less downfield shifted (vertical lines between spectra vi and vii) and broadened. The presence of major and minor Trp resonances suggest the presence of two or more conformations, a feature observed also in the upfield aliphatic spectrum of I68 (Supplementary Data).

M64I impairs nuclear localization

Studies employed an SRY-β-galactosidase fusion plasmid to direct nuclear localization of β-galactosidase enzymatic activity (Figure 7(a)).[34,35] A control for loss of C-NLS activity was provided by the previously characterized R133W variant.[35] Transient transfection experiments were performed using COS-7 cells to enable comparison with prior studies,[34,35] and a male rat gonadal-ridge embryogenic cell line (CH34 cells)[49] to provide a physiologically appropriate milieu. Cellular localization of β-galactosidase was evaluated quantitatively by staining of fixed cells using 5-bromo-4-chloro-3-

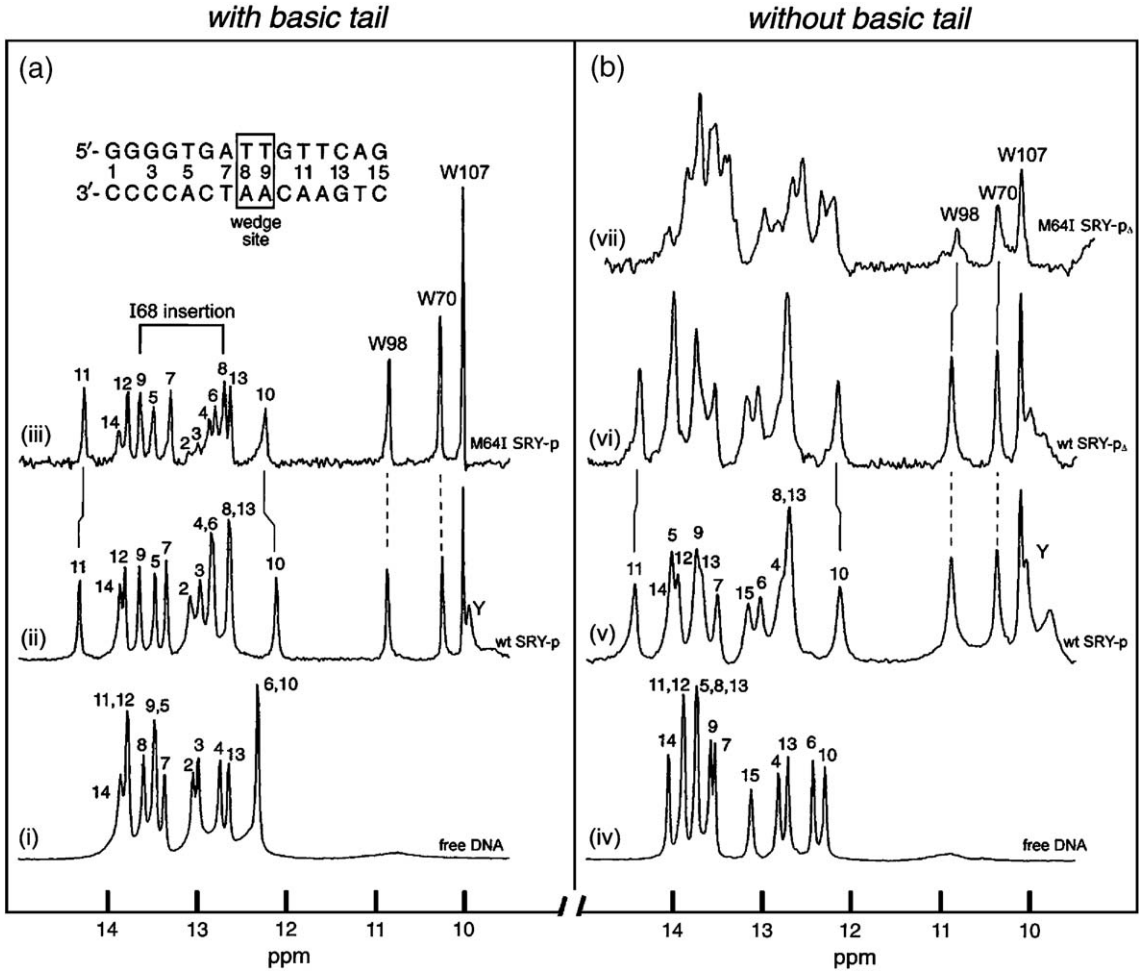

Figure 6. ^{1}H-NMR studies of SRY-DNA complexes. (a) Binding of tailed SRY domains to 15 bp consensus DNA site (inset at top). (i) free DNA imino resonances (12–14 ppm) at 25 °C; assignments as indicated. Broadening of G1 and G15 terminal resonances is due to DNA fraying. (ii and iii) Marked changes in imino chemical shifts in specific 1:1 complexes with wt SRY-p (ii) and M64I SRY-p (iii). Although changes are similar in the two complexes, a trend toward smaller shifts is observed for the M64I complex (vertical lines; Supplementary Data). Resonances T8 and T9 at the site of I68 insertion are indicated. Trp indole NH resonances in complexes (10–11 ppm) exhibit essentially identical chemical shifts and line-widths. (b) Binding of truncated SRY domains to 12 bp consensus DNA site (base-pairs 4–15 of the site in (a)). (iv) Free DNA imino resonances (12–14 ppm) at 25 °C; assignments as indicated. Base-pairs are numbered according to the 15 bp site; i.e. from 4–15. (v) The wt SRY-p complex. (vi) The wt SRY-p$_{\Delta}$ complex. (vii) The M64I SRY-p$_{\Delta}$ complex. Spectra i–iv were obtained at 500 MHz; spectra v–vii were obtained at 400 MHz. Solvent excitation was avoided by the use of a shifted shaped pulse, except in spectrum iii, which employed a flip-back pulse scheme. Attenuation of protected *para*-OH resonance of Y74 in spectrum iii (labeled Y in (ii))[46] is due to additional T_2 relaxation during flip-back sequence.

indolyl-β-D-galactosidase (X-gal). About 200 cells were counted in each case by X-gal staining (Figure 7(a)); the results are summarized as a histogram (Figure 7(b) and (c)). Representative images of transfected COS-7cells are shown in the upper row of Figure 7(a), and CH34 cells in the lower row. In accord with the results of earlier studies[35] wt SRY directs exclusive nuclear localization of β-galactosidase in *ca.* ~86% of COS-7 cells (186 of 216 cells counted; photomicrograph i in Figure 7(a)) and 80% of CH34 cells (153 of 192 cells; photomicrograph i′) whereas variant R133W yields a broad distribution of β-galactosidase in >84% of COS-7 cells (169 of 202 cells counted; image ii) and ~88% of CH34 cells (162 of 184 cells; image ii′).

The M64I SRY fusion protein likewise gives rise to both pan-cellular and cytoplasmic distributions in ~80% of cells analyzed in either cell line (146 of 216 COS-7 cells counted and 160 of 206 CH34 cells; images iii and iii′ in Figure 7(a)); differences between cell lines are not of statistical significance. A similar impairment in nuclear localization was observed in studies of an M64A SRY fusion protein (Supplementary Data), suggesting that defective nuclear import reflects a loss of an M64-dependent mechanism and not gain of an aberrant I64-related function. Partial nuclear import of the M64I-SRY or M64A-SRY fusion proteins presumably reflects continued activity of C-NLS but impaired interaction of N-NLS with a protein required for complete

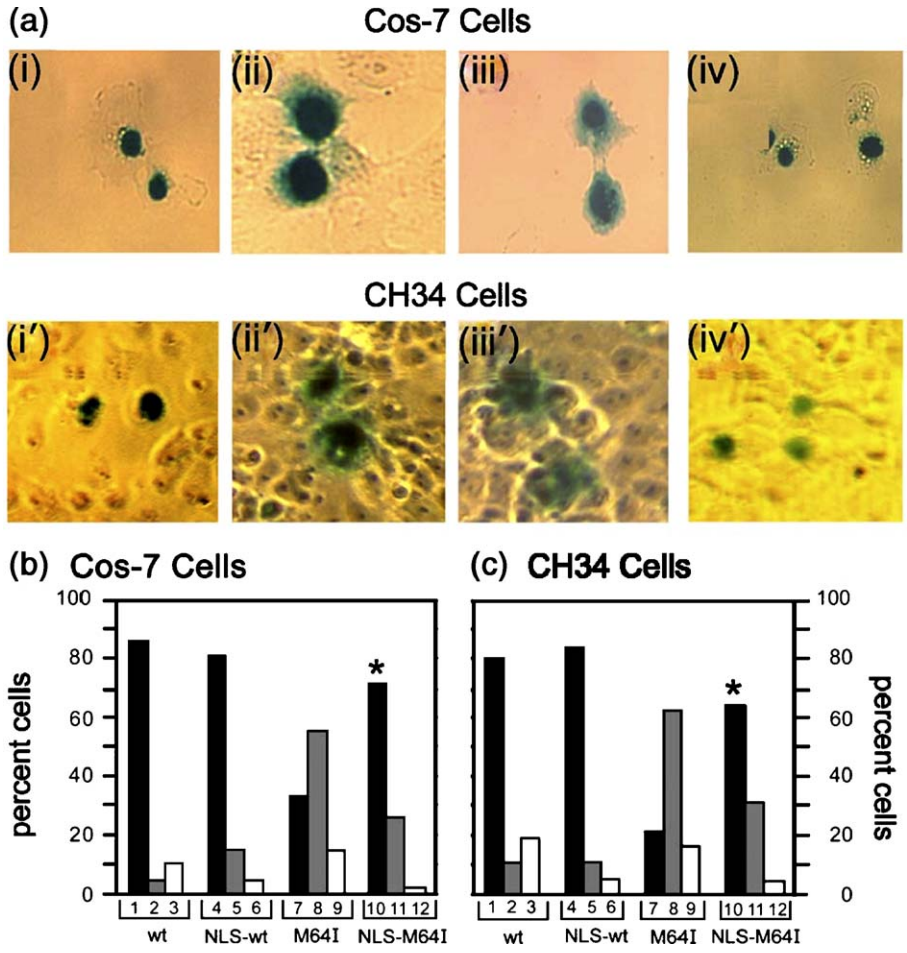

Figure 7. M64I impairs nuclear localization. (a) Sub-localization distribution of SRY-β-galactosidase fusion protein in COS-7 cells (top row) and CH34 cells (bottom row) before and after addition of universal NLS. Representative photomicrographs: (i and i′, wt SRY) nuclear, (ii and ii′, R133W) pancellular, (iii and iii′, M64I) pancellular, and (iv and iv′, SV40 NLS-M64I) nuclear. (b) and (c) Histograms depicting percentage subcellular distribution in (b) COS-7 cells and (c) CH34 cells: in each panel (columns 1–3) wt, (4–6) SV40 NLS-wt, (7–9) M64I, (10–12) SV40 NLS-M64I-SRY. Columns 1, 4, 7 and 10 designate the percentage of transfected cells with a nuclear staining pattern; columns 2, 5, 8 and 11 designate the percentage with pancellular pattern; and columns 3, 6, 9 and 12, designate the percentage with a cytoplasmic pattern. Asterisks indicate rescue of nuclear localization of the M64I-SRY-β-galactosidase fusion protein by heterologous NLS.

nuclear localization. Although N-NLS does not bind to importin α or β,[58] Harley and co-workers have proposed that its function is mediated by CaM binding.[38] Accordingly, we investigated whether M64I impairs SRY-CaM binding or perturbs the structure of their complex (Supplementary Data). CaM-SRY binding was monitored *via* a GMSA in which the specific SRY–p/DNA complex is inhibited progressively by formation of a competing SRY-p/CaM complex. In this assay, developed by Harley and colleagues,[39] CaM is equipotent in disrupting the wt and M64I complexes. In addition, respective structures of the wt and variant SRY-p/CaM complexes, as probed by CD, were indistinguishable. Further, the microenvironments of Trp residues in the two complexes were found to be similar, as probed by acrylamide fluorescence quenching. Although the identity of the M64I-sensitive N-NLS interacting partner is not known, addition of a heterologous NLS (the canonical basic cluster in simian virus 40 (SV40) large T antigen)[44] at the N terminus of the M64I SRY fusion protein restores efficient nuclear import (asterisks in Figure 7(b) and (c)): staining was exclusively nuclear in 128 of 178 COS-7 cells and 79 of 122 CH34 cells (images iv and iv′ in Figure 7(a)). The SV40 NLS does not affect nuclear import of the wt SRY fusion protein, itself competent for nuclear localization (columns 4 in Figure 7(b) and (c)).

On nuclear import M64I SRY exhibits native gene-regulatory activity

A luciferase-based assay in CH34 cells, employing transient co-transfection of SRY expression and reporter plasmids into CH34 cells, provides a model for SRY-activated transcription.[49] Although not physiological, such activation is specific to SRY and its consensus target sequences rather than a structure-specific DNA-binding activity, as indicated

by the inactivity of high-mobility group protein HMGB2; furthermore, architectural transcription factors with different DNA sequence specificities (LEF-1 and IRE-ABP) are only weakly active.[48] In this assay, it was shown previously that the M64I mutant fails to activate transcription.[49] To distinguish whether this loss of activity is due to perturbations in DNA-binding properties or to inefficient nuclear import, we investigated the effect of the mutation following rescue of nuclear localization by the SV40 NLS. Whereas the heterologous NLS has no effect on the activity of wt SRY in either CH34 or COS-7 cells (columns 4 and 4′ in Figure 8(b)), engineered nuclear localization of the M64I variant restores activation of luciferase in both cell lines (red asterisks in Figure 8(b)).

To extend these results to a physiological model of SRY-directed transcriptional activation, we developed a real-time PCR (RT-Q-rtPCR) assay for transcriptional activation of the endogenous *Sox9* genes in CH34 cells by transfected human *SRY* or variant *SRY* alleles (see Materials and Methods). Design of this assay recapitulates the role of the SRY-SOX9 pathway in the overall program of testis determination (Figure 8(a)). Transient transfection of wt SRY (efficiency ~15% based on control co-transfection of *lacZ* expressing β-galactosidase) activates transcription of *Sox9* and *Mullerian inhibiting substance* (*Mis*) but not endogenous rat genes encoding β-actin, Sry, or other Sox factors unrelated to testis determination (Sox2, Sox3, Sox4, Sox5, and Sox10).[16] Baseline expression of the endogenous *Sox9* alleles is shown in Figure 8(c) in untransfected cells (column 7) and on transfection of either an empty vector (column 8) or the R133W variant SRY (column 9). Transient transfection of wt SRY activates *Sox9* by about sixfold relative to these vector controls (Figure 8(c), columns 10 and 7).

Such activation is unaffected by the SV40 NLS (Figure 8(c), column 11). In the RT-Q-rtPCR assay as in the above luciferase assay, M64I leads to reduced activation of *Sox9* (Figure 8(c), column 12). The extent of reduction is similar to, but less marked than, that caused by R133W. Strikingly, engineered nuclear import of the M64I fusion protein restores a wild-type level of *Sox9* activation (red asterisk above column 13 in Figure 8(c)). Essentially identical results are obtained with M64A (Supplementary Data). Western blot controls verify in each case that the wt and variant epitope-tagged SRY proteins are expressed at equal concentrations. Rescue of the transcriptional activity of M64I SRY on nuclear localization suggests that in the patient gonadal dysgenesis is due to impaired nuclear localization. Such rescue also indicates that subtle changes in the architecture of a consensus DNA complex, or the more marked perturbations observed in non-consensus complex, are either not relevant to, or do not impair the mechanism of, transcriptional activation in these assays.

Discussion

Sexual dimorphism provides a model of a genetic switch between alternative programs of development.[59] Studies of human intersex abnormalities highlight the importance of sequence-specific DNA-bending proteins: clinical mutations in either *Sry*[4,8,42,49] or *Sox9*[20–22] are associated with pure gonadal dysgenesis leading to XY somatic sex reversal. The structure of an SRY–DNA complex provides a basis for analysis of these clinical mutations.[43] The present study has focused on the role of M64, part of a conserved set of non-polar residues at the crux of the angular surface of the HMG box. Designated the hydrophobic wedge, these side-chains (consensus residues M9, F12, I13 and W43 in the HMG box) pack across the minor groove between AT base-pairs (bold; 5′A**TT**GTT-3′ and complement). The wedge is a hotspot for clinical mutations.[5,60] M64 packs at the periphery of the wedge, near (but not in intimate association with) the DNA surface.

Local models of wedge–DNA deformation

Why wedge mutations might affect DNA bending seems apparent: packing of the wedge (with partial intercalation of the I68 cantilever) disrupts base-stacking but not base-pairing (Figure 1(b)).[57] Although overall bending is distributed along the underwound DNA (Figure 2(a)), the unstacked AT base-pairs define a discontinuity in double-helical axis, defining a discrete locus of DNA bending (Figure 2(c)).[43] Indeed, differences between wt and M64I complexes are largely localized to the wedge–DNA motif, leading to altered bending at the ApA cantilever site (Figure 2(c) and (d)). Enhanced bending in the wt complex is proposed to reflect steric repulsion of the dexoyribose moiety of the second adenine base by the M64 sulfur atom (gold in Figure 2(c)), in turn constrained by a hydrogen bond from R72 (arrowhead). This hydrogen bond is absent from the M64I complex (Figure 2(d)): as a consequence, R72 is displaced, and the dexoyribose moieties of the splayed adenosine bases are less effectively braced by the smaller I64 γ-CH_3 group. Resulting decreases in respective roll and tilt angles at the ApA step by 8° and 5°, respectively, account for the 13° difference in bending between complexes.[43] Thus, the perturbation in the M64I SRY–DNA complex is a molecular ''sin of omission'', as native DNA bending is not enforced as effectively by the variant brace. This analysis, parsing a DNA-bending defect to the special properties of a single wt sulfur atom, provides a tour de force of molecular reductionism.

Reassessment reveals non-local coupling within bent complex

We were motivated by two considerations to reinvestigate the DNA-bending properties of M64I

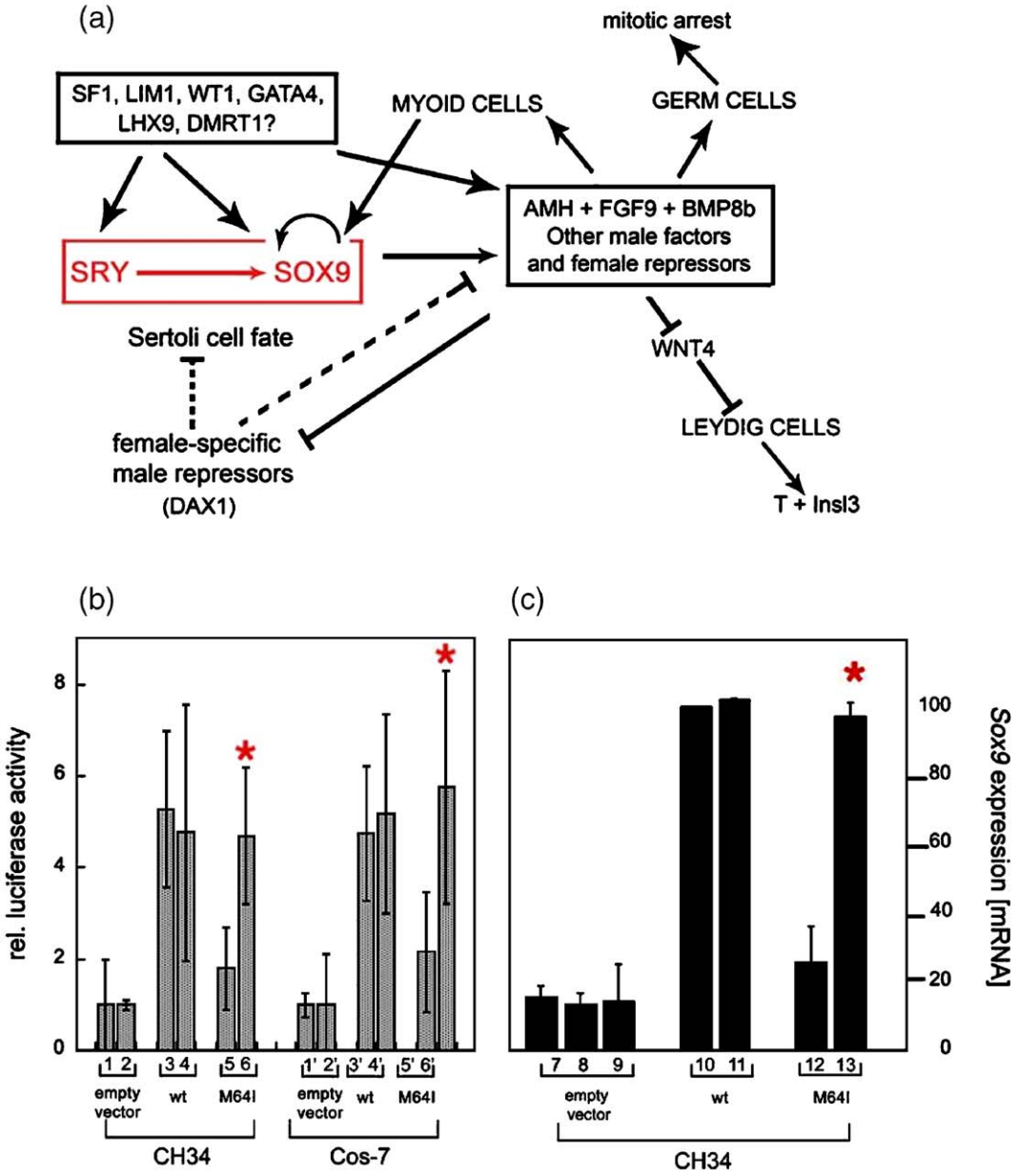

Figure 8. Pathway of SRY-regulated testicular differentiation and transcription assays. (a) Genetic interactions during male sex determination: the SRY-SOX9 pathway (red box) is essential for testis formation. Although it is not known whether SRY activates *SOX9* directly or indirectly, these factors both act within supporting cell lineage to direct Sertoli cell differentiation and signal to the other lineages. Factors at the lower left are anti-testis genes, ensuring that the central pathway does not operate in XX gonads (broken lines). T, testosterone; Insl3, insulin-related peptide. The Figure is adapted from Lovell-Badge.[14] (b) and (c) Transient-transfection transcriptional assays demonstrate that the decreased activity of M64I SRY is restored on fusion of a heterologous NLS. (b) Luciferase assay following co-transfection of SRY expression and 5′-ATTGTT-dependent reporter plasmids in CH34 cells (columns 1–6; left) and COS-7 cells (columns 1′–6′; right). Columns 1, 2, 1′ and 2′, empty-vector control; columns 3, 4, 3′ and 4′, wt SRY construct; and columns 5, 6, 5′ and 6′, M64I SRY construct. SV40 NLS is added to the construct in the second column in each case; columns 2, 4, 6, 2′, 4′, and 6′. Red asterisks indicate restoration of transcriptional activation by the fused SV40 NLS. Error bars indicate standard deviation of three replicates. (c) Real-time rt-PCR assay of endogenous *Sox9* expression in CH34 cells. Values are normalized to wt SRY-driven expression of *Sox9* (100%). Columns 7 and 8 indicate baseline expression of *Sox9* on transfection of empty plasmid (column 7) or endogenous expression (column 8); column 9 is the expression of R133W variant; columns 10 and 11, wt SRY and SV40 NLS SRY; and columns 12 and 13, M64I SRY and SV40 NLS M64I SRY. Error bars indicate standard deviation of three replicates. The red asterisks indicate restoration of *Sox9* expression to that of wild-type on fusion of the SV40 NLS.

SRY. First, the original PGE studies employed a fragment of the HMG box (SRY-p_Δ) lacking part of the basic tail.[42] The corresponding wt fragment exhibits altered DNA-binding and DNA-bending properties relative to a tailed domain (SRY-p): the latter resembles intact SRY, whereas SRY-p_Δ exhibits twofold lower DNA binding and reduced DNA bending.[46] The decrement of 7–10° observed by PGE on binding of respective SRY domains to a high-affinity DNA site is increased to 19° in complexes containing variant DNA *site 4*,[46] as employed in structural studies.[43] Whereas the 5′-T→A transversion in site 4 (5′-**T**TTGTG-3′) enhances DNA bending slightly,[42] the 3′-T→G transversion (5′-TTTGT**G**-3′) attenuates DNA bending markedly in both tailed and truncated complexes.[46] Reassessment of M64I SRY was further motivated by studies of murine Sox2 as, surprisingly, the homologous substitution in its HMG box (M47I in intact Sox2) was found to cause no change in specific DNA bending.[61] This absence of perturbation seemed anomalous, given the otherwise similar DNA-binding and DNA-bending properties of Sox2 and SRY.[61]

The apparent discordance between the effects of homologous wedge mutations in SRY and Sox2 led Scaffidi and Bianchi to conclude that the mechanism of Sox2–DNA recognition must differ, at least in part, from that of SRY.[61] We noticed, however, that the Sox2 domain employed in these studies contained a complete C-terminal tail and utilized consensus DNA sites, suggesting that the apparent differences might have other explanations. Indeed, recent structures of Sox2–DNA complexes (as visualized within ternary Sox2–POU–DNA assemblies) are essentially identical with the SRY–DNA complex, including homologous wedge–DNA deformations.[62,63] Such correspondence is consistent with conservation of respective protein–DNA interfaces: only four out of 27 DNA contact residues in Sox2 differ from those of SRY, and these appear to be conservative changes.[63] Interestingly, in such ternary assemblies the Sox2 tail binds within the DNA minor groove (as in SRY) and mediates protein–protein contacts to the POU domain.[62,63]

We have demonstrated here that binding of the basic tail of the SRY HMG box restores near-native DNA bending to M64I in the canonical DNA complex. Defective DNA bending by M64I SRY is nonetheless unmasked by DNA transversions in the tail-binding site (see below). The original bending defect[42] was, in retrospect, an unfortunate consequence of protein truncation; at the time of these studies, the role of the tail and the precise extent of the SRY DNA-binding domain were not well understood. The present results thus resolve the apparent contradiction between the effects of homologous mutations in SRY and Sox2,[61] but raise a salient question with respect to prior structural analysis: how can tail-dependent rescue of DNA bending be reconciled with the elegant structural explanation of impaired M64 SRY–DNA bending ascribed to the absence of the M64 sulfur atom?[43] We suggest that binding of the tail within the minor groove downstream of the wedge stabilizes an overall DNA conformation ''tuned'' to the native DNA bend angle. Induced fit of the protein–DNA complex may exhibit long-range coupling *via* successive contiguous protein elements: immobilization of the tail may stabilize the minor wing of the HMG box and, in turn, the wedge–DNA interface. It is possible that tail binding constrains the conformation of DNA base-pairs in immediate contact, leading to propagated effects on roll and tilt angles at the splayed ApA wedge step. Given transmission of tail-dependent constraints, it is noteworthy that in the structure of the variant complex,[43] I64 permits decreased DNA bending merely through ineffective DNA bracing rather than active specification of a novel bend angle (see above). This sin of omission is compensated by the tail in the tuned complex. The similar properties of M64I and M64A variants suggest that the more marked loss of side-chain volume in the Ala variant can likewise be well tolerated in a tailed DNA complex.

The tail-tuning model is supported by observations that restoration of native bending to M64I SRY complexes requires a canonical 5′-ATTGTT-3′ DNA site: defects in DNA bending are observed in complexes containing lower-affinity and less bendable sites. An example is provide by site 5, which contains core element 5′-ATTG**A**T-3′ and complement (substitution in bold).[49] We speculate that the T→A transversion (incompatible with random-binding site selection data[64] and inconsistent with known SOX target sites,[65]) impairs binding of the tail and/or interrupts the transmission of conformational constraints from tail to wedge. Comparison of wt and M64I SRY-site 5 complexes in essence recapitulates (indeed, aggravates) the DNA bending defect originally associated with use of truncated protein fragments.[42] An analogous but less marked perturbation is observed in complexes containing variant site 4 (5′-**T**TTGT**G**-3′). This site permits tail binding as explicitly characterized in structural studies (Figure 2).[43] It would be of interest to redetermine the structures of wt and M64I SRY–DNA complexes as bound to a consensus DNA site.

A distinct mechanism of tail-dependent tuning of DNA architecture is observed in lymphoid enhancer factor 1 (LEF-1; also designated T-cell factor 1, TCF-1). Unlike the SRY tail, the LEF-1 tail folds back across the major groove near the center of the DNA bend.[66] This difference may account for the sharper bend angle of the LEF-1 complex (~120°).[47,66–70] The basic side-chains of the LEF-1 tail, although not well ordered, provide a set of positive charges within the crux of the compressed major groove, effectively alleviating electrostatic repulsion in the DNA that would otherwise oppose DNA bending.[66] By contrast, because compression of the major groove is less marked in the SRY complex, such electrostatic stabilization is apparently not required in the major groove. Whereas truncation of the LEF-1 tail attenuates DNA binding and bending dramatically, the effects of

truncation of the SRY tail on the wt complex are modest.[46] Unlike the wt SRY complex, the conformational stability of the M64I SRY complex hinges on the tail, as indicated by NMR and time-resolved FRET measurements. Of particular interest, analysis of the distribution of end-to-end distances in the bound DNA (Figure 4(d)) indicates that tail truncation broadens the range of bend angles in an ensemble of M64I complexes; no such effect is observed in the wt ensemble.[46] It is possible that the broad conservation of Met at HMG box position 9 of SRY, Sox, and LEF-1 factors relates, in part to its bracing function in non-consensus DNA complexes, however dispensable this brace appears to be in a consensus DNA complex. Such a structural role might serve to expand the range of DNA regulatory sequences regulated by these architectural factors.

Impaired nuclear localization masks native transcriptional activation

Whereas previous studies of M64I SRY sought to rationalize gonadal dysgenesis at the atomic level,[42,43] an alternative perspective arises from cell biology: M64I SRY exhibits an unexpected defect in nuclear localization. Nuclear import of wt SRY is directed by two NLS elements (one at each end of the HMG box),[32,34] coordinately required for complete nuclear localization.[35] Whereas C-NLS (a cluster of basic tail residues) binds to importin β and thus relates to a well-established mechanism of nuclear import,[37] N-NLS (a bipartite basic motif)[32] does not bind to importin α or to importin β.[36] Although its import is instead proposed to be mediated by CaM,[38] evidence for this proposal is only circumstantial. In the present study, we have shown that M64I does not alter the affinity or structure of the SRY–CaM complex (Supplementary Data). The sensitivity of nuclear localization to an aliphatic substitution at a neutral site between the paired basic clusters is unusual, and its molecular mechanism poses an interesting future problem.[71,72]

Previous studies of M64I SRY in cell culture demonstrate an impaired ability to activate the transcription of a reporter gene in a co-transfection assay.[49] These studies were limited by the lack of clear relationship between the assay and physiological gene regulation and by the absence of controls to characterize effects of mutations on nuclear localization.[48] We have demonstrated here that the transcriptional activity of M64I SRY is restored on rescue of nuclear localization by fusion of a heterologous NLS. Further, wt activity is observed in a male embryonic gonadal-cell assay designed to recapitulate a critical early step in Sertoli cell differentiation: direct or indirect transcriptional activation of *Sox9* following expression of *Sry* in the differentiating gonadal ridge.[18,19] The RT-Q-rtPCR assay employs transient transfection of wt or mutant SRY in CH34 cells,[49] followed by monitoring of the mRNA levels of endogenous genes. Changes in the concentration of *Sox9* mRNA are sensitive to mutations in SRY. Rescue of M64I SRY-directed *Sox9* activation by fusion of the SV40 NLS strongly suggests that sex reversal in this clinical setting is due to impaired nuclear localization and not to small changes in specific DNA affinity or bending. The more marked perturbations unmasked in non-consensus complexes, although of structural interest, do not correlate with impaired *Sox9* activation and hence must be peripheral to its mechanism of gene regulation.

DNA bending and the male-specific transcriptional program

The original report of XY sex reversal associated with a selective defect in SRY-directed DNA bending[42] suggested a mechanistic relationship between DNA architecture and gene regulation.[27] Indeed, in related systems, decreased DNA bending has been observed to impair transcriptional regulation. An example is provided by LEF-1: its HMG box bends the wild-type TCRα enhancer element by 120-130°),[66–68] whereas functional analysis of nucleotide substitutions in this element has shown that variant target sites bent to 90° exhibit impaired transcriptional activation uncorrelated with effects on protein binding.[69] Similar studies of amino acid substitutions in the HMG box of SOX2 and nucleotide substitutions in its target site have demonstrated that spatially precise DNA bending is essential to the transcriptional regulation of a target gene.[61] Future characterization of SRY target genes may enable analogous studies to determine architectural requirements of SRY-mediated transcriptional regulation. The present reassessment of M64I SRY does not exclude the discovery of mutations at other sites at which gonadal dysgenesis might correlate with a selective perturbation in DNA bending. In the absence of such clinical mutations, it would be of interest to investigate the relationship between DNA architecture and testicular differentiation in gonadal cell culture and in transgenic murine models of SRY-directed XX sex reversal.[13,14,45] We speculate that SRY-directed testicular differentiation requires DNA bending within a critical range tuned to the structural requirements of enhanceosome assembly.

Materials and Methods

Plasmids

Bacterial and mammalian expression plasmids were constructed as described.[35,48] All constructions were verified by DNA sequencing.

Protein purification

Intact SRY and its domains were expressed in *Escherichia coli* strain BL21 (DE3)pLysS and purified as described.[45]

Purity was >98% as assessed by PAGE. Results of mass spectrometry were in accord with expected values.

DNA-binding assay

GMSA employed a 36 bp consensus DNA site (5′-CATACTGCGGGGGTG ATTGTT CAGGATCATAC-TGCG-3′ and complement) as described.[45]

DNA-bending assay

DNA sites containing the SRY binding sites were cloned between XbaI and SalI sites of pBend2.[73] Probes of equal length, with the binding site at various distances from the ends, were generated by PCR and employed in PGE studies as described.[45]

SRY–calmodulin binding assays

Binding of SRY to CaM (from Sigma-Aldrich, Inc. St. Louis, MO) was monitored by GMSA and intrinsic Trp fluorescence as described.[38,39] Structures of wt and M64I SRY-p/CaM complexes were probed by Trp fluorescence and acrylamide quenching as described,[38] using an ATF 105 fluorimeter (Aviv Biomedical, Lakewood, NJ) and further characterized by CD (below).

Circular dichroism

Spectra were obtained at 20° C in a 1 mm path-length quartz cuvette using an Aviv spectropolarimeter (Aviv Biomedical., Lakewood, New Jersey). Thermal unfolding and guanidine denaturation were monitored at 222 nm in 10 mM potassium phosphate (pH 7.4), 140 mM KCl as described.[45]

Fluorescence spectroscopy

FRET studies employed a 15 bp DNA duplex (5′-TCGGTG*ATTGTT*CAG-3′ and complement; consensus target site underlined) as described.[45] Distance distributions were obtained from simultaneous global analysis of experimental fluorescence decay curves using the Marquardt non-linear least-squares method.[53] Steady-state FRET-based titration experiments were used to determine dissociation constants (K_d) at 15 °C as described.[46]

NMR spectroscopy

Spectra of free domains were observed at 25 °C in (a) 10 mM deuterated acetic acid (pH 4.5), 140 mM KCl and in (b) 10 mM potassium phosphate (pH 7.4), 140 mM KCl. The spectra of DNA complexes were obtained at 25 °C in 10 mM potassium phosphate (pH 6.0), 50 mM KCl. Assignments were obtained as described.[43,57,74]

Cell culture

CH34 cells were kindly provided by P. K. Donahoe (Massachusetts General Hospital); COS-7 cell lines are from the American Type Culture Collection. Cells were cultured in Dulbecco's modified Eagle's medium (DMEM) containing 5% (v/v) heat-inactivated fetal bovine serum and penicillin/streptomycin (Life Technologies, Inc) at 37 °C under 5% (v/v) CO_2. Transient transfections were performed using lipofectAMINE™2000 kit (Life Technologies, Inc). After screening conditions for 1 h, 2 h, 4 h, and 6 h of transfection, a time of 2 h was chosen as the optimal time for β-galactosidase staining. For luciferase and *Sox9* Rt-PCR assays, identical concentrations of plasmid were used: 1 μg of DNA/2×10^6 cells for the β-galactase study; 1 μg of DNA /1×10^6 cells for *Sox9* rt-PCR and 1 μg of DNA (1:1 ratio of SRY plasmid to reporter plasmid) /2×10^6 cells for the luciferase assay).

Cellular localization studies

The wt SRY-β-galactosidase construct was kindly provided by G. Scherer (University of Freiburg, Germany). In NLS fusion proteins, a heterologous element (PKKKRK) encoded by a DNA segment was inserted 3′ to the SRY start codon. Cells were fixed with 4% (v/v) paraformaldehyde in phosphate-buffered saline, stained for 2 h with X-gal, and assessed by using a Zeiss inverted microscope (Germany) as described.[35] The Pearson correlation method was used to assess possible pair-wise relationships; $p<0.05$ (two tailed) was employed as a threshold for statistical significance.

Transcriptional activation assays

Luciferase co-transfection assays were performed as described.[48] The RT-Q-rtPCR *Sox9* assay employed 50 μl PCR reaction mixtures, containing 25 μl of 2× SYBR green (BioRad), 500 nM each primer, 1 μg of RNA extract and 1 μl of iScript reverse transcriptase™. The first real-time PCR step was 10 min at 50 °C and 5 min at 95 °C, followed by 45 cycles of denaturation for 10 s at 95 °C and annealing/extension for 30 s at 55 °C. The fluorescent signal intensities were recorded and analyzed during PCR in an ABI Prism 7700 sequence detector system (Applied Biosystems) using the SDS (Ver. 1.91) software. Dissociation curves for SOX9 were generated after each run to confirm that the increased fluorescence intensities were not attributable to non-specific signals (primer-dimers). C_T values within the linear exponential increase phase were used to measure the original mRNA template copy numbers and to construct the calibration curve according to the formula (copies/ml = $6.023\times 1023\times[C\times A_{260}$/molecular mass). Assays were performed in triplicate; both western blots and rt-PCR were performed in each case to normalize the quantity of expressed SRY.

Acknowledgements

We thank H. Chen, C.-Y. King, C. Kung, L. A. Labeots, J. Radek, and E. Rivera for participation in the early stages of this work; Professor P. K. Donahoe, H.-Y. Kao, D. Samols, and E. Stavnezer for discussions; Q. X. Hua for molecular graphics; and S. Price for assistance with the manuscript. This work was supported, in part, by an equipment grant from the Israel Science Foundation to E.H. (number 553-99), a grant from the United States/Israel Binational Foundation (E.H. and M.A.W.; number

98-362) and in its early stages by the National Institutes of Health (M.A.W.; GM051558). These studies are a contribution from the Cleveland Center for Structural Biology.

Supplementary Data

Supplementary data associated with this article can be found, in the online version, at doi:10.1016/j.jmb.2006.04.048

References

1. Sinclair, A. H., Berta, P., Palmer, M. S., Hawkins, J. R., Griffiths, B. L., Smith, M. J. *et al.* (1990). A gene from the human sex-determining region encodes a protein with homology to a conserved DNA-binding motif. *Nature*, **346**, 240–244.
2. Gubbay, J., Collignon, J., Koopman, P., Capel, B., Economou, A., Munsterberg, A. *et al.* (1990). A gene mapping to the sex-determining region of the mouse Y chromosome is a member of a novel family of embryonically expressed genes. *Nature*, **346**, 245–250.
3. Ner, S. S. (1992). HMGs everywhere. *Curr. Biol.* **2**, 208–210.
4. Berta, P., Hawkins, J. R., Sinclair, A. H., Taylor, A., Griffiths, B. L., Goodfellow, P. N. & Fellous, M. (1990). Genetic evidence equating SRY and the testis-determining factor. *Nature*, **348**, 448–450.
5. McElreavy, K., Vilain, E., Abbas, N., Costa, J. M., Souleyreau, N. Kucheria, K. *et al.* (1992). XY sex reversal associated with a deletion 5′ to the SRY ''HMG box'' in the testis-determining region. *Proc. Natl Acad. Sci. USA*, **89**, 11016–11020.
6. Hawkins, J. R., Taylor, A., Berta, P., Levilliers, J., Van der Auwera, B. & Goodfellow, P. N. (1992). Mutational analysis of SRY: nonsense and missense mutations in XY sex reversal. *Hum. Genet.* **88**, 471–474.
7. Harley, V. R., Jackson, D. I., Hextall, P. J., Hawkins, J. R., Berkovitz, G. D., Sockanathan, S. *et al.* (1992). DNA binding activity of recombinant SRY from normal males and XY females. *Science*, **255**, 453–456.
8. Vilain, E., Jaubert, F., Fellous, M. & McElreavey, K. (1993). Pathology of 46, XY pure gonadal dysgenesis absence of testis differentiation associated with mutations in the testis-determining factor. *Differentiation*, **52**, 151–159.
9. Koopman, P., Gubbay, J., Vivian, N., Goodfellow, P. & Lovell-Badge, R. (1991). Male development of chromosomally female mice transgenic for Sry. *Nature*, **351**, 117–121.
10. Whitfield, L. S., Lovell-Badge, R. & Goodfellow, P. N. (1993). Rapid sequence evolution of the mammalian sex-determining gene SRY. *Nature*, **364**, 713–715.
11. Ferrari, S., Harley, V. R., Pontiggia, A., Goodfellow, P. N., Lovell-Badge, R. & Bianchi, M. E. (1992). SRY, like HMG1, recognizes sharp angles in DNA. *EMBO J.* **11**, 4497–4506.
12. Mitchell, C. L. & Harley, V. R. (2002). Biochemical defects in eight SRY missense mutations causing XY gonadal dysgenesis. *Mol. Genet. Metab.* **77**, 217–225.
13. Bergstrom, D. E., Young, M., Albrecht, K. H. & Eicher, E. M. (2000). Related function of mouse SOX3, SOX9, and SRY HMG domains assayed by male sex determination. *Genesis*, **28**, 111–124.
14. Lovell-Badge, R., Canning, C. & Sekido, R. (2002). *Sex-determining Genes in Mice: Building Pathways,* John Wiley and Sons Ltd, West Sussex, UK.
15. Werner, H. M., Huth, J. R., Gronenborn, A. M. & Clore, G. M. (1995). Molecular basis of human 46X,Y sex reversal revealed from the three-dimensional solution structure of the human SRY-DNA complex. *Cell*, **81**, 705–714.
16. Wegner, M. (1999). From head to toes: the multiple facets of Sox protein. *Nucl. Acids Res.* **6**, 1409–1420.
17. Koopman, P. (1999). Sry and Sox9: mammalian testis-determining genes. *Cell Mol. Life Sci.* **55**, 839–856.
18. Sekido, R., Bar, I., Narvaez, V., Penny, G. & Lovell-Badge, R. (2004). SOX9 is up-regulated by the transient expression of SRY specifically in Sertoli cell precursors. *Dev. Biol.* **274**, 271–279.
19. Beverdam, A. & Koopman, P. (2006). Expression profiling of purified mouse gonadal somatic cells during the critical time window of sex determination reveals novel candidate genes for human sexual dysgenesis syndromes. *Hum. Mol. Genet.* **15**, 417–431.
20. Foster, J. W. & Graves, J. A. (1994). An SRY-related sequence on the marsupial X chromosome: implications for the evolution of the mammalian testis-determining gene. *Proc. Natl Acad. Sci. USA,* **91**, 1927–1931.
21. Wagner, T., Wirth, J., Meyer, J., Zabel, B., Held, M. Zimmer, J. *et al.* (1994). Autosomal sex reversal and campomelic dysplasia are caused by mutations in and around the SRY-related gene SOX9. *Cell*, **79**, 1111–1120.
22. Kwok, C., Weller, P., Guioli, S., Foster, J. W., Mansour, S. Zuffardi, O. *et al.* (1995). Mutations in SOX9, the gene responsible for campomelic dysplasia and autosomal sex reversal. *Am. J. Hum. Genet.* **57**, 1028–1036.
23. Canto, P., Vilchis, F., Soderlund, D., Reyes, E. & Mendez, J. P. (2005). A heterozygous mutation in the desert hedgehog gene in patients with mixed gonadal dysgenesis. *Mol. Hum. Reprod.* **11**, 833–836.
24. Colvin, J. S., Green, R. P., Schmahl, J., Capel, B. & Ornitz, D. M. (2001). Male-to-female sex reversal in mice lacking fibroblast growth factor 9. *Cell*, **104**, 875–889.
25. Bouma, G. J., Albrecht, K. H., Washburn, L. L., Recknagel, A. K., Churchill, G. A. & Eicher, E. M. (2005). Gonadal sex reversal in mutant Dax1 XY mice: a failure to upregulate Sox9 in pre-Sertoli cells. *Development*, **132**, 3045–3054.
26. Barrionuevo, F., Bagheri-Fam, S., Klattig, J., Kist, R., Taketo, M. M., Englert, C. & Scherer, G. (2006). Homozygous inactivation of Sox9 causes complete XY sex reversal in mice. *Biol. Reprod.* **74**, 195–201.
27. Bewley, C. A., Gronenborn, A. M. & Clore, G. M. (1998). Minor groove-binding architectural proteins: structure, function, and DNA recognition. *Annu. Rev. Biophys. Biomol. Struct.* **27**, 105–131.
28. Weiss, M. A. (2005). Molecular mechanisms of male sex determination: the enigma of SRY. In *DNA Conformation and Transcription* (Ohyama, T., ed), pp. 1–15, Landes Bioscience, Georgetown, TX.
29. Matsuzawa-Watanabe, Y., Inoue, J. & Semba, K. (2003). Transcriptional activity of testis-determining factor SRY is modulated by the Wilms' tumor 1 gene product, WT1. *Oncogene*, **22**, 7900–7904.
30. Oh, H. J., Li, Y. & Lau, Y. (2005). Sry associates with the heterochromatin protein 1 complex by interacting with a KRAB domain protein. *Biol. Reprod.* **72**, 407–415.

31. Furumatsu, T., Tsuda, M., Yoshida, K., Taniguchi, N., Ito, T. Hashimoto, M. *et al.* (2005). Sox9 and p300 cooperatively regulate chromatin-mediated transcription. *J. Biol. Chem.* **280**, 35203–35208.
32. Poulat, F., Girard, F., Chevron, M. P., Goze, C., Rebillard, X. Calas, B. *et al.* (1995). Nuclear localization of the testis determining gene product SRY. *J. Cell. Biol.* **128**, 737–748.
33. Salas-Cortes, L., Jaubert, F., Barbaux, S., Nessmann, C., Bono, M. R. Fellous, M. *et al.* (1999). The human SRY protein is present in fetal and adult Sertoli cells and germ cells. *Int. J. Dev. Biol.* **43**, 135–140.
34. Sudbeck, P. & Scherer, G. (1997). Two independent nuclear localization signals are present in the DNA-binding high-mobility group domains of SRY and SOX9. *J. Biol. Chem.* **272**, 27848–27852.
35. Li, B., Zhang, W., Chan, G., Jancso-Radek, A., Liu, S. & Weiss, M. A. (2001). Human sex reversal due to impaired nuclear localization of SRY. A clinical correlation. *J. Biol. Chem.* **276**, 46480–46484.
36. Forwood, J. K., Harley, V. & Jans, D. A. (2001). The C-terminal nuclear localization signal of the sex-determining region Y (SRY) high mobility group domain mediates nuclear import through importin beta 1. *J. Biol. Chem.* **276**, 46575–46582.
37. Harley, V. R., Layfield, S., Mitchell, C. L., Forwood, J. K., John, A. P. Briggs, L. J. *et al.* (2003). Defective importin beta recognition and nuclear import of the sex-determining factor SRY are associated with XY sex-reversing mutations. *Proc. Natl Acad. Sci. USA,* **100**, 7045–7050.
38. Sim, H., Rimmer, K., Kelly, S., Ludbrook, L. M., Clayton, A. H. A. & Harley, V. R. (2005). Defective calmodulin-mediated nuclear transport of the sex-determining region of the Y chromosome (SRY) in XY sex reversal. *Mol. Endocrinol.* **19**, 1884–1892.
39. Harley, V. R., Lovell-Badge, R., Goodfellow, P. N. & Hextall, P. J. (1996). The HMG box of SRY is a calmodulin binding domain. *FEBS Letters*, **391**, 24–28.
40. Harley, V. R., Clarkson, M. J. & Argentaro, A. (2003). The molecular action and regulation of the testis-determining factors, SRY (sex-determining region on the Y chromosome) and SOX9 [SRY-related high-mobility group (HMG) box 9]. *Endocr. Rev.* **24**, 466–487.
41. Prieve, M. G., Guttridge, K. L., Munguia, J. & Waterman, M. L. (1998). Differential importin-alpha recognition and nuclear transport by nuclear localization signals within the high-mobility-group DNA binding domains of lymphoid enhancer factor 1 and T-cell factor 1. *Mol. Cell. Biol.* **18**, 4819–4832.
42. Pontiggia, A., Rimini, R., Harley, V. R., Goodfellow, P. N., Lovell-Badge, R. & Bianchi, M. E. (1994). Sex-reversing mutations affect the architecture of SRY-DNA complexes. *EMBO J.* **13**, 6115–6124.
43. Murphy, E. C., Zhurkin, V. B., Louis, J. M., Cornilescu, G. & Clore, G. M. (2001). Structural basis for SRY-dependent 46-X,Y sex reversal: modulation of DNA bending by a naturally occurring point mutation. *J. Mol. Biol.* **312**, 481–499.
44. Nakanishi, M., Eguchi, A., Akuta, T., Nagoshi, E., Fujita, S. Okabe, J. *et al.* (2003). Basic peptides as functional components of non-viral gene transfer vehicles. *Curr. Protein Pept. Sci.* **4**, 141–150.
45. Phillips, N. B., Nikolskaya, T., Jancso-Radek, A., Ittah, V., Jiang, F. Singh, R. *et al.* (2004). Sry-directed sex reversal in transgenic mice is robust to enhanced DNA bending: comparison of human and murine in HMG boxes. *Biochemistry*, **43**, 7066–7081.
46. Phillips, N. B., Jancso-Radek, A., Ittah, V., Singh, R., Chan, G., Haas, E. & Weiss, M. A. (2006). SRY and human sex determination: the basic tail of the HMG box functions as a kinetic clamp to augment DNA bending. *J. Mol. Biol.* **358**, 172–192.
47. Giese, K., Kingsley, C., Kirshner, J. R. & Grosschedl, R. (1995). Assembly and function of a TCR alpha enhancer complex is dependent on LEF-1-induced DNA bending and multiple protein-protein interactions. *Genes Dev.* **9**, 995–1008.
48. Ukiyama, E., Jancso-Radek, A., Li, B., Milos, L., Zhang, W. Phillips, N. B. *et al.* (2001). SRY and architectural gene regulation: the kinetic stability of a bent protein-DNA complex can regulate its transcriptional potency. *Mol. Endocrinol.* **15**, 363–377.
49. Haqq, C. M., King, C. Y., Ukiyama, E., Falsafi, S., Haqq, T. N., Donahoe, P. K. & Weiss, M. A. (1994). Molecular basis of mammalian sexual determination: activation of Mullerian inhibiting substance gene expression by SRY. *Science*, **266**, 1494–1500.
50. Haas, E. & Katchalski-Katzir, I. Z. (1978). Effect of the orientation of donor and acceptor on the probability of energy transfer involving electronic transitions of mixed polarization. *Biochemistry*, **17**, 5064–5070.
51. Parkhurst, K. M., Brenowitz, M. & Parkhurst, L. J. (1996). Simultaneous binding and bending of promoter DNA by the TATA binding protein: real time kinetic measurements. *Biochemistry*, **35**, 7459–7465.
52. Murphy, E. C., Zhurkin, V. B., Louis, J. M., Cornilescu, G. & Clore, G. M. (2001). Structural basis for SRY-dependent 46-X,Y sex reversal: modulation of DNA bending by a naturally occurring point mutation. *J. Mol. Biol.* **312**, 481–499.
53. Beechem, J. M. & Haas, E. (1989). Simultaneous determination of intramolecular distance distributions and conformational dynamics by global analysis of energy transfer measurements. *Biophys. J.* **55**, 1225–1236.
54. Haas, E. (1997). The problem of protein folding and dynamics: time resolved dynamic non-radiative excitation energy transfer measurements. *IEEE-JSTC*, **2**, 1088.
55. Dragan, A. I., Read, C. M., Makeyeva, E. N., Milgotina, E. L., Churchill, M. E., Crane-Robinson, C. & Privalov, P. L. (2004). DNA binding and bending by HMG boxes: energetic determinants of specificity. *J. Mol. Biol.* **343**, 371–393.
56. Weiss, M. A. (2001). Floppy SOX: mutual induced fit in HMB (High-Mobility Group) Box-DNA recognition. *Mol. Endocrinol.* **15**, 353–362.
57. King, C. Y. & Weiss, M. A. (1993). The SRY high-mobility-group box recognizes DNA by partial intercalation in the minor groove: a topological mechanism of sequence specificity. *Proc. Natl Acad. Sci. USA,* **90**, 11990–11994.
58. Preiss, S., Argentaro, A., Clayton, A., John, A., Jans, D. A. Ogata, T. *et al.* (2001). Compound effects of point mutations causing campomelic dysplasia/autosomal sex reversal upon SOX9 structure, nuclear transport, DNA binding, and transcriptional activation. *J. Biol. Chem.* **276**, 27864–27872.
59. Goodfellow, P. N. & Lovell-Badge, R. (1993). SRY and sex determination in mammals. *Annu. Rev. Genet.* **27**, 71–92.
60. Scherer, G., Held, M., Erdel, M., Meschede, D., Horst, J., Lesniewicz, R. & Midro, A. T. (1998). Three novel SRY mutations in XY gonadal dysgenesis and the enigma of XY gonadal dysgenesis cases without SRY mutations. *Cytogenet. Cell Genet.* **80**, 188–192.

61. Scaffidi, P. & Bianchi, M. E. (2001). Spatially precise DNA bending is an essential activity of the Sox2 transcription factor. *J. Biol. Chem.* **276**, 47296–47302.
62. Remenyi, A., Lins, K., Nissen, L. J., Reinbold, R., Scholer, H. R. & Wilmanns, M. (2003). Crystal structure of a POU/HMG/DNA ternary complex suggests differential assembly of Oct4 and Sox2 on two enhancers. *Genes Dev.* **17**, 2048–2059.
63. Williams, D. C. J., Cai, M. & Clore, G. M. (2004). Molecular basis for synergistic transcriptional activation by Oct1 and Sox2 revealed from the solution structure of the 42-kDa Oct1.Sox2.Hoxb1-DNA ternary transcription factor complex. *J. Biol. Chem.* **279**, 1449–1457.
64. Harley, V. R., Lovell-Badge, R. & Goodfellow, P. N. (1994). Definition of a consensus DNA binding site for SRY. *Nucl. Acids Res.* **22**, 500–501.
65. Mertin, S., McDowall, S. G. & Harley, V. R. (1999). The DNA-binding specificity of SOX9 and other SOX proteins. *Nucl. Acids Res.* **27**, 1359–1364.
66. Love, J. J., Li, X., Case, D. A., Giese, K., Grosschedl, R. & Wright, P. E. (1995). Structural basis for DNA bending by the architectural transcription factor LEF-1. *Nature*, **376**, 791–795.
67. Giese, K., Cox, J. & Grosschedl, R. (1992). The HMG domain of lymphoid enhancer factor 1 bends DNA and facilitates assembly of functional nucleoprotein structures. *Cell*, **69**, 185–195.
68. Read, C. M., Cary, P. D., Preston, N. S., Lnenicek-Allen, M. & Crane-Robinson, C. (1994). The DNA sequence specificity of HMG boxes lies in the minor wing of the structure. *EMBO J.* **13**, 5639–5646.
69. Giese, K., Pagel, J. & Grosschedl, R. (1997). Functional analysis of DNA bending and unwinding by the high mobility group domain of LEF-1. *Proc. Natl Acad. Sci. USA*, **94**, 12845–12850.
70. Lnenicek-Allen, M., Read, C. M. & Crane-Robinson, C. (1996). The DNA bend angle and binding affinity of an HMG box increased by the presence of short terminal arms. *Nucl. Acids Res.* **24**, 1047–1051.
71. Chook, Y. & Blobel, G. (2001). Karyopherins and nuclear import. *Curr. Opin. Struct. Biol.* **11**, 703–715.
72. Hirano, K., Zeng, Y., Hirano, M., Nishimura, J. & Kanaide, H. (2003). Sequence requirement for nuclear localization and growth inhibition of p27Kip1R, a degradation-resistant isoform of p27Kip1. *J. Cell Biochem.* **89**, 191–202.
73. Kim, J., Zwieb, C., Wu, C. & Adhya, S. (1989). Bending of DNA by gene-regulatory proteins: construction and use of a DNA bending vector. *Gene*, **85**, 15–23.
74. Werner, M. H., Bianchi, M. E., Gronenborn, A. M. & Clore, G. M. (1995). NMR spectroscopic analysis of the DNA conformation induced by the human testis determining factor SRY. *Biochemistry*, **34**, 11998–12004.
75. Desclozeaux, M., Poulat, F., de Santa Barbara, P., Capony, J. P., Turowski, P., Jay, P. *et al.* (1998). Phosphorylation of an N-terminal motif enhances DNA-binding activity of the human SRY protein. *J. Biol. Chem.* **273**, 7988–7995.
76. Poulat, F., Barbara, P. S., Desclozeaux, M., Soullier, S., Moniot, B. Bonneaud, N. *et al.* (1997). The human testis determining factor SRY binds a nuclear factor containing PDZ protein interaction domains. *J. Biol. Chem.* **272**, 7167–7172.
77. Thevenet, L., Albrecht, K. H., Malki, S., Berta, P., Boizet-Bonhoure, B. & Poulat, F. (2005). NHERF2/SIP-1 interacts with mouse SRY via a different mechanism than human SRY. *J. Biol. Chem.* **280**, 38625–38630.
78. Maniatis, T., Falvo, J. V., Kim, T. H., Kim, T. K., Lin, C. H., Parekh, B. S. & Wathelet, M. G. (1998). Structure and function of the interferon-beta enhanceosome. *Cold Spring Harbor Symp. Quant. Biol.* **63**, 609–620.

Edited by J. O. Thomas

(Received 13 March 2006; received in revised form 18 April 2006; accepted 20 April 2006)
Available online 9 May 2006